

Short-term CO₂ emissions forecasting based on decomposition approaches and its impact on electricity market scheduling

Neeraj Bokde^a, Bo Tranberg^b, Gorm Bruun Andresen^{a,*}

^a*Department of Engineering - Renewable Energy and Thermodynamics, Aarhus University, 8000, Denmark*

^b*Ento Labs ApS, Inge Lehmanns Gade 10, 6, 8000, Aarhus C, Denmark*

Abstract

The world is facing major challenges related to global warming and emissions of greenhouse gases is a major causing factor. In 2017, energy industries accounted for 46% of all CO₂ emissions globally, which shows a large potential for reduction. This paper proposes a novel short-term CO₂ emissions forecast to enable intelligent scheduling of flexible electricity consumption to minimize the resulting CO₂ emissions. Two proposed time series decomposition methods are developed for short-term forecasting of the CO₂ emissions of electricity. These are in turn bench-marked against a set of state-of-the-art models. The result is a new forecasting method with a 48-hour horizon targeted the day-ahead electricity market. Forecasting benchmarks for France show that the new method has a mean absolute percentage error that is 25% lower than the best performing state-of-the-art model. Further, application of the forecast for scheduling flexible electricity consumption is studied for five European countries. Scheduling a flexible block of 4 hours of electricity consumption in a 24 hour interval can on average reduce the resulting CO₂ emissions by 25% in France, 17% in Germany, 69% in Norway, 20% in Denmark, and just 3% in Poland when compared to consuming at random intervals during the day.

Keywords: forecasting, CO₂ emission, demand flexibility

*Corresponding author

Email address: gba@eng.au.dk (Gorm Bruun Andresen)

1. Introduction

The modern human society is facing many challenges related to global warming and emissions of greenhouse gases into the atmosphere is a major factor responsible for it [1, 2].

According to a report by the European Commission, in 2017 China was responsible for 29% of total CO₂ emission and surpassed other economies including the USA, Europe, and India which contributed 14%, 10%, and 7%, respectively [3]. Further, this report revealed that the global annual CO₂ emissions and global per capita emissions have climbed to 37 billion metric tons and 4.9 metric tons in the year 2014, respectively. In the same year, energy industries accounted for 46% of all CO₂ emissions globally [4]. This shows a large potential for reduction.

In 2009, most countries have shown their intentions to reduce CO₂ emission at the Copenhagen Global Climate Conference (also known as the 2009 United Nations Climate Change Conference) [5]. During this conference, the European Union and the USA committed to lowering the CO₂ emission by 20 to 30% and 4% of the level in 1990, respectively. Whereas, by 2020, the developing economies, China and India targeted reducing the CO₂ emissions per GDP by around 40% and 25% of the level in 2005 by 2020, respectively. Furthermore, most countries as a united globe have set the targets for upcoming decades to reduce greenhouse gases significantly [6]. In addition to this, the Paris agreement (famously named as 20/20/20) set to reduce CO₂ emissions by 20%, increase the renewable energy share by 20%, and increase energy efficiency by 20% for the whole World [7]. The country-wise profiles related to CO₂ emissions and climate change are discussed in detail by the CarbonBrief team [8].

During recent years, most countries targeted specific CO₂ emissions to meet global warming challenges. This leads to lots of research contributions on the trends of CO₂ emissions to assist energy planning policies. Although, there are

numerous techniques proposed by research teams throughout the World. Ye et. al. [9] roughly categorized these techniques into two forms, namely, target decomposition and policy evaluation. Target decomposition is a simple and easy technique, which decomposes the targeted goals of CO₂ emissions into sub-divisions. These sub-divisions can be based on various criteria based on different departments or provinces [10, 11]. However, these studies quantify the potential of a specific policy. Whereas, in policy evaluation techniques, policies to reduce CO₂ emissions are evaluated under present scenarios. These techniques include statistical, econometric and computer simulation approaches to forecast CO₂ emissions.

Forecasting CO₂ intensity and related CO₂ emissions is important today and will become urgent in the future to recommend effective CO₂ emissions reduction policies to the policymakers. Furthermore, it may aid the system in integrating renewable energy. Most countries are now under tremendous pressure to limit reduce their CO₂ emissions. Hence, it is of great importance to explore and analyze the responsible factors for CO₂ emissions. Accurate forecasting models enable such analyses.

Throughout Europe, there are multiple bidding areas in many countries in the day-ahead electricity market. For each bidding area, the transmission capacity availabilities vary and this may congest the power flow between neighboring bidding areas. Such congestion leads to differences in the price between bidding areas. Among the energy markets in Europe are Nord Pool covering Scandinavian countries [12], and EPEX SPOT covering North-West Europe [13].

The purpose of electricity markets is price formation to establish equilibrium between supply and demand. This is done on an hourly level in the day-ahead market for electricity. The day-ahead market clears at noon and provides an hourly price for the 24 hours of the following day based on matching bids and offers received from producers and consumers. When bidding, one needs to specify the amount of energy in MWh for an hour to be bought (consumed) or sold (produced) at a certain price level (Eur/MWh) for the next

day.

Consider the time framework as shown in Figure 1 for further understanding of the electricity market bidding. So far, such time frameworks have been used to plan the market price forecast in the day-ahead energy market. In Figure 1, the day ($D + 1$), i.e. tomorrow, is the forecasting period of interest and for this auction, the consumer needs to bid before 12.00 AM today, i.e. day D . In addition, considering some buffer periods and time to place bids in the market, it will be better for the consumer to be ready with such a forecast analysis at 09:00 - 10.00 AM on the day D . Hence, this day ahead electricity market needs 12-36 hours, hourly resolved forecasts.

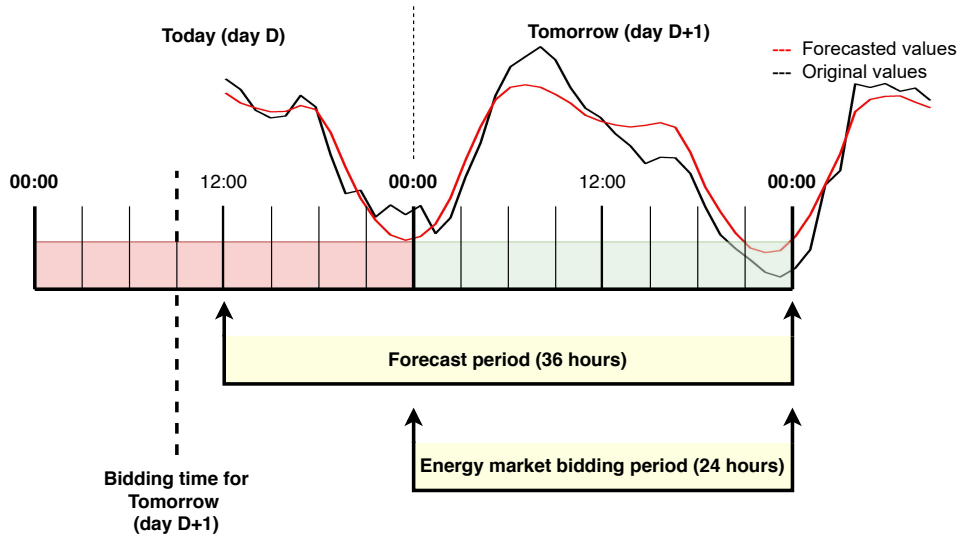


Figure 1: Time framework to forecast for the day-ahead energy market.

Normally, consumers schedule the time slots with reference to electricity prices and it is based on the electricity prices forecasts. The motivation is to reduce the overall cost of consumed electricity for the desired scheduled period [14].

In recent years many countries, public buildings, public infrastructures, and institutes started to take initiatives to understand the sources and the nature of the energy they are consuming. Such entities want to keep track of their

CO₂ emissions. In relation to energy consumption, this means focusing on greener energy with lower CO₂ intensity. In the case of bidding in the day-ahead market, the consumer could schedule not just after the forecasted price, but also accordingly to forecasted CO₂ intensity as a primary or secondary objective. However, this can only be achieved if appropriate forecasts of the CO₂ is available. With this motivation in mind, this study investigates new, appropriate models for electricity bidding-friendly multi-step hours CO₂ emissions forecasts.

From a system perspective, forecasts like the one proposed in this study are important for the scheduling of flexible electricity consumption to have an effect on the increasing integration of renewable energy resources in the electricity system. Flexible consumers must be able to place bids in the day-ahead market to provide timely signals for the market participants e.g., to adjust production plans accordingly.

In this article, two time series decomposition methods are compared for short-term forecasting of the CO₂ emissions of electricity. First, the CO₂ intensities are obtained using the power flow tracing technique presented in [15] and combined with country-specific average CO₂ intensity per generation technology as proposed in [16]. Second, these intensity time series are decomposed into three components with two approaches. Finally, three different forecasting models are employed to predict all components, and these predicted magnitudes are combined to obtain the final forecasted values for a given CO₂ intensity series. The performance of both decomposition approaches is then compared with several state-of-the-art forecasting methods. The CO₂ intensity series exhibit non-stationary and nonlinear patterns, which are forecasted effectively and precisely with the multi-scale integrated prediction methods.

Related studies in the literature focus on long-term forecasts of CO₂ emissions. For electricity consumers to be able to provide flexible demand to the system they need more accurate short-term forecasts as the novel methods we are proposing in this study. Though these new methods are short-term forecasts, they predict values that are 36 to 48 hours ahead in time in a single

step, which is a novel approach for this application. Consequently, this paper contributes to the literature as follows:

- The models to forecast the short-term CO₂ intensity time-series for 36–48 hours ahead values, which are necessary for electricity market bidding.
- Discussing the impact of forecasted CO₂ emissions on the electricity market schedule.
- Enabling flexible electricity consumption scheduling to minimize CO₂ emissions.

The remainder of this article is organized as follows: Section 2 discusses the motivation behind 48 steps ahead forecasting of CO₂ intensity and its effects on electricity markets. Section 3 provides a precise review of various models employed for CO₂ intensity forecasting. The proposed methodology along with two decomposition strategies are discussed in Section 4. Further, the performance evaluation of the proposed methods is studied on sample standard data sets in Section 5. In Section 6, a case study is discussed which evaluates the performance of the proposed methods for short-term multi-step CO₂ intensity data set forecasting. Section 7 presents a case study on potential CO₂ emissions reductions resulting from scheduling flexible electricity consumption. Finally, the conclusions of the paper are summarized in Section 8. All abbreviations and variables used throughout the paper are listed in Table 1.

2. Method

2.1. Review of CO₂ emissions forecasts

Long-term CO₂ emissions forecasting enables policymakers and planners to estimate and reduce the future carbon footprint. However, the short-term CO₂ emissions forecasting is critical to understand how much CO₂ will be emitted so that e.g., producers and consumers of electricity can schedule their production and consumption to minimize their resulting emissions.

Table 1: Nomenclature.

Abbreviations		Variables	
ARIMA	AutoRegressive Integrated Moving Average	$x(t)$	a time series
CO2	Carbon Dioxide	$C_i(t)$	i^{th} IMF
DK	Denmark	$r_m(t)$	the final residual
DPSF	Differenced Pattern Sequence-based Forecasting method	$e_L(t)$	Lower envelope
EEMD	Ensemble Empirical Mode Decomposition	$e_H(t)$	Upper envelope
EMD	Empirical Mode Decomposition	$a(t)$	Average of lower and upper envelopes
ENTSO-E	European Network of Transmission System Operators for Electricity	M	Ensemble numbers
EPEX SPOT	European Power Exchange	e	Amplitude of the white noise series
FFNN	Feedforward Neural Network	e'	Final standard deviation of error
GDP	Gross Domestic Product	X_i	Observed data
HVAC	Heating, Ventilation, and Air Conditioning	\hat{X}_i	Forecasted data
IMF	Intrinsic Mode Functions	N	Number of time steps for forecast evaluation
IPT	Integrated Powertrain		
kWh	Kilo-Watt Hour		
LSSVM	Least-squares support-vector machine		
LSTM	Long-Short-Term Memory		
MAE	Mean Absolute Error		
MAPE	Mean Absolute Percentage Error		
max. LE	Maximum Lyapunov Exponent		
MWh	Mega-Watt Hour		
NWP	Numerical Weather Prediction		
PSF	Pattern Sequence-based Forecasting method		
RMSE	Root Mean Square Error		
SOPR	Second-Order Polynomial Regression		
SVM	Support Vector Machine		

Globally, long-term CO₂ emissions have been an attractive topic for research and discussion, but there are very few articles discussing short-term forecasting. Finenko et. al. [17] is one of the initial articles which analyzed the hourly patterns of CO₂ emissions for electricity generation and stated that most CO₂ emissions reduction can be achieved during day time with a case study of Singapore. Mason et. al. [18] proposed a case study in Ireland, which successfully forecasts short-term CO₂ emissions using evolutionary neural networks. There are few case studies [19, 20, 21] which predicted air pollutants and ozone concentrations for short time horizons, which were closely related to carbon footprints. Similarly, a light-use-efficiency model based on numerical weather prediction (NWP) method is proposed for short-term forecasting of CO₂ fluxes in Europe [22].

For the first time, grid CO₂ intensity in support of heating, ventilation, and air-conditioning (HVAC) load is forecasted for the day ahead horizon by [23]. This study foresees the opportune time of the day for carbon saving based on CO₂ intensity forecasts and accordingly shutdown of the HVAC plant.

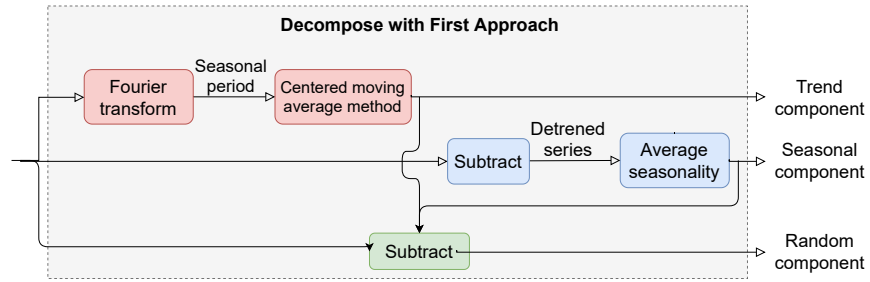
In contrast to the CO₂ emissions time series used for long-term forecasting, the one used for short-term forecasting is of higher complexity. For short-term forecasting, the data set used has an hourly resolution, hence it exhibits rapidly changing patterns. This highly chaotic time series is challenging to forecast with the standard set of forecasting methods. As discussed in the literature review, the models used for long-term CO₂ emissions forecasting were mainly focused on understanding and estimating the trends of the time series. However, in time series used for short-term forecasting, there are many components apart from trends, which need to be considered. Generally, a series can be segmented into three parts; these are the seasonal, trend and random components. The seasonal component shows the patterns in the series that repeat with a fixed period, whereas the trend component shows the tendency of a series to increase or decrease over a long period of time, which is a smoother, general and long-term tendency. Finally, the random component is purely irregular in nature. It does not represent any pattern and hence is an uncontrollable

and unpredictable part of the series. Minimizing the share of the random component, the time series becomes more informative and non-chaotic in nature. Since all these components individually have different patterns, it is not adequate to handle them jointly with a single forecasting model as it is important to analyze the behavior of each component individually.

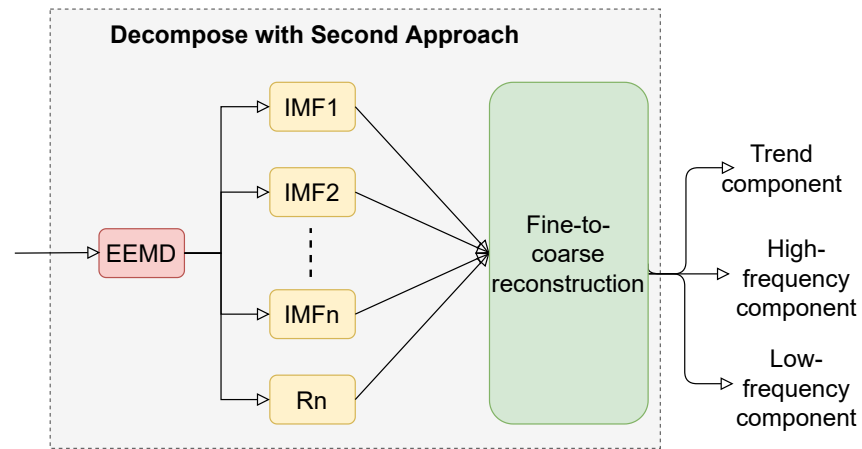
In the present study, the time series is decomposed into the seasonal, trend and random component series with two different approaches, and these components are further forecasted with different models. Eventually, forecasts of CO₂ intensity are achieved and a comparison of the mentioned decomposition approaches is done.

2.2. Decomposition with first approach

The first approach is a basic and well-known methodology, which first derives the trend, seasonal and noise components one by one with various statistical steps. The first step is to detect the trend in the time series using the centered moving average method. In this step, a moving window with the length of the seasonal period of the time series is used. The seasonality of a time series is either observed by a seasonal period of the time series (daily, weekly, monthly, or yearly) or estimated using the Fourier transform method. Then, this moving window is replaced with the average of the window and the trend series is obtained. The second step is detrending the time series by removing the trend series obtained in the first step from the original time series. The detrended series appears to be seasonal but infected with a noise component. Now, to determine the actual seasonality component, the average seasonality needs to be calculated. It is obtained in the third step by adding seasonality of the detrended series together and dividing it by the seasonality period. In the final step, the random noise component is extracted by subtracting seasonal and trend components from the original time series. The block-diagram of this approach is as shown in Figure 2a.



(a) Decomposition with moving averages.



(b) Decomposition with EEMD method.

Figure 2: Block diagram of the (a) moving averages and (b) EEMD method based decomposition approaches.

2.3. Decomposition with second approach

Furthermore, the second approach is based on a decomposition methodology. This ensemble empirical mode decomposition (EEMD) method is used to decompose the time series into a number of sub-series. It is a modification of the EMD method, which is an empirical and effective decomposition method with a less complex procedure. EMD is efficient at handling non-linear and non-stationary time series. The methodology was introduced by [24] and since then, it has become increasingly popular in the research field of forecasting, and substantially enhancing prediction process [25]. With the methodology, the time series is decomposed into numerous intrinsic mode functions (IMF) and one residual. The process is termed as the EMD sifting process and can be expressed linearly as:

$$x(t) = \sum_{i=1}^m C_i(t) + r_m(t) \quad (1)$$

where, m is the number of IMFs, $C_i(t)$ is the i th IMF at the time t , and $r_m(t)$ is the final residual of the time series $x(t)$. All $C_i(t)$ have zero means and are nearly orthogonal to each other [26].

In the processes, firstly all local minima and maxima values of $x(t)$ are identified. Then the cubic spline interpolation is used to obtain the lower envelope $e_L(t)$ and upper envelop $e_H(t)$ for the minima and maxima values. The average value of $a(t)$ of the lower and upper envelope is calculated as:

$$a(t) = \frac{(e_L(t) + e_H(t))}{2}. \quad (2)$$

The first component $d(t)$ is given by:

$$d(t) = x(t) - a(t). \quad (3)$$

After the above step, if $d(t)$ meets the IMF properties, then it is considered as the first IMF. Otherwise, $x(t)$ is replaced by $d(t)$, and the above process is repeated. In case of the residual function $r(t)$, when it becomes monotonic

or only extreme values are present from which no more IMF is achieved, the process is terminated [27]. The IMF should satisfy the following two condition:

- The number of extrema and zero crossings of the data set must either be equal or differ at most by one.
- At any point, the mean value defined by $e_L(t)$ and $e_H(t)$ should be zero.

The EEMD method is an adaptive approach developed from EMD. It was proposed by [28]. The methodology has an improvement over EMD, as it adds finite white noise to the original data, to overcome the problem of mode mixing that exists with EMD. In the mode mixing problem, the data may not decompose properly and hence a similar scale series are found to exist in different IMFs [26], which results in loss of physical meaning in them. To decompose the time series by EEMD the following steps have been adopted [28]: Random white noise having zero mean and given standard deviation e has to be added to the available time series $x(t)$.

This time series is decomposed into various IMFs and one residual component. The above procedure is repeated with different white noise series each time. The mean of corresponding IMFs of the decomposition is obtained as the final results. The addition of all the IMFs will not be the same at the end [29]. The effect of white noise can be minimized based on the following equation [28] and [30].

$$e' = \frac{e}{\sqrt{M}}, \quad (4)$$

where M is the ensemble numbers, e is the amplitude of the added white noise series, and e' is the final standard deviation of error. Many researchers have supported the use of EEMD for the decomposition of time series and it has been implemented successfully in various fields [31].

The case studies in [32] and [33] applied EEMD to time series of carbon and crude oil prices and decomposed them into three IMF components: high frequency, low frequency, and trend as shown in Figure 2b. These components

seem equivalent, but an alternative to the seasonality, noise, and trend components, respectively. A fine-to-coarse reconstruction algorithm [33] is used to separate the IMFs into high- and low-frequency components, whereas the residual is the trend component. In this procedure, the mean of the algorithm is traced and when it departs significantly from zero for the ' n 'th IMF, the partial reconstruction using IMF1-IMF($n - 1$) represents the high-frequency component. Whereas IMF n to the last IMF comprises the low-frequency component. The detailed analysis is further discussed in the following sections for the proposed case study.

2.4. Significance of decomposition in forecast

The significance of decomposition methods in a forecasting model can be explained with human experience and observations. Consider an example of weather in a particular region. If one observed extreme cold in December and excessive rainfall in August every year, this suggests that next year, there will be another colder December as well as sufficient rain in August. Similarly, the decomposed seasonal component captures the seasonal patterns which repeat after a specific time interval and a forecasting model can easily observe and estimate the future within such seasonal or high-frequency component series.

Again, though it is expected, extreme cold in December sometimes is delayed or the extreme cold peak is not occurring in a particular year. Besides, sometimes, unexpected rainfall is observed in the winter season. All these unexpected observations are nothing but the random activities based on various natural or unnatural processes of the Earth. The random or low-frequency components obtained with the discussed decomposition approaches represent this random behavior of the time series.

Further, climate change is another example. Earlier studies [34, 35] confirms significant increase in temperature during decades as shown in Figure 3. The broad sense of temperature change in the century represented a trend line. Again, these trend series can help a forecasting model to estimate such long-term behavior present in the time series. Both discussed decomposition

approaches generate trend components with different strategies.

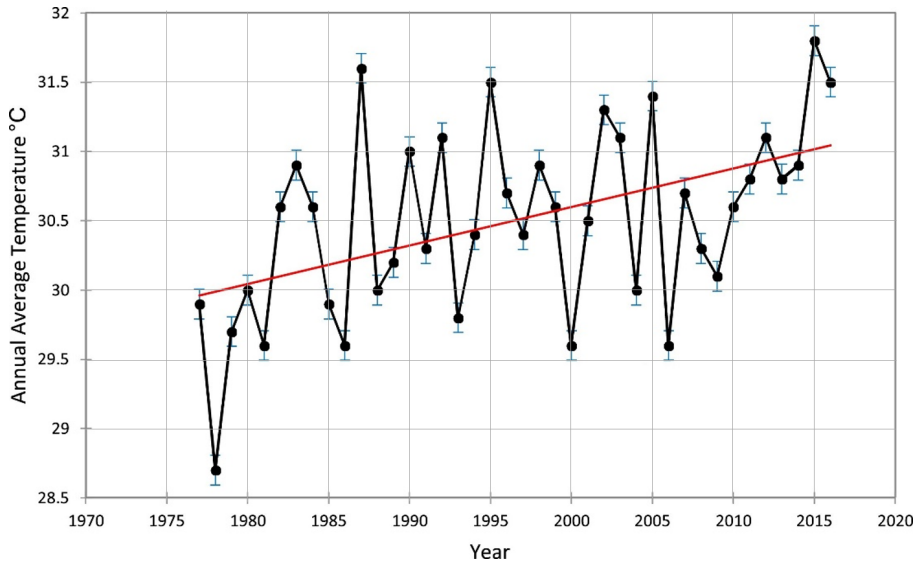


Figure 3: A trend showing annual average temperature for years 1977–2016 (Source: [35])

In this way, a proper strategy to forecast each of the series (seasonal, trend, and random components) individually with distinct suitable models may better reproduce the respective patterns in the forecasted series. Eventually, a more accurate forecast can be achieved.

2.5. Selection of forecasting models

After decomposing the time series with both approaches, as shown in Figure 4, the decomposed component forecasting method is selected for each. The forecasted values are then aggregated to produce the final forecast results for the original time series as described in Figure 5. The first and second decomposition-based forecasting methods are shown in Figure 5 (a) and (b), respectively.

Now, the selection of the forecasting models for each component is a crucial process. A cross-validation approach is adopted to decide the most suitable forecasting model for each decomposed component obtained in the discussed decomposition methods. The data set used for this purpose is from the West

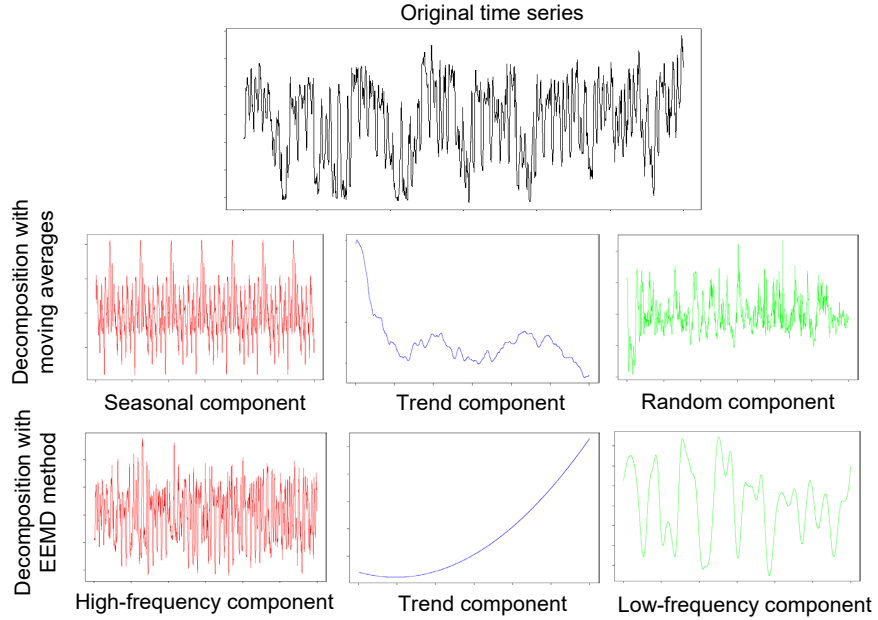


Figure 4: Decomposed components with both approaches.

Denmark price area (DK-1), which is the same as discussed in detail in subsequent Section 6. Ten continuous patches of time series with the length of 1200 samples are selected randomly with the Monte-Carlo strategy and decomposed into three components with both approaches as discussed in earlier sections. These components are forecasted for the next 48 values with ARIMA, FFNN, PSF, and DPSF models. Throughout the article, the comparisons of accuracies of forecasting models are executed with three error metrics; RMSE, MAE, and MAPE, which are given as:

$$\text{RMSE} = \sqrt{\frac{1}{N} \sum_{i=1}^N |X_i - \hat{X}_i|^2} \quad (5)$$

$$\text{MAE} = \frac{1}{N} \sum_{i=1}^N |X_i - \hat{X}_i| \quad (6)$$

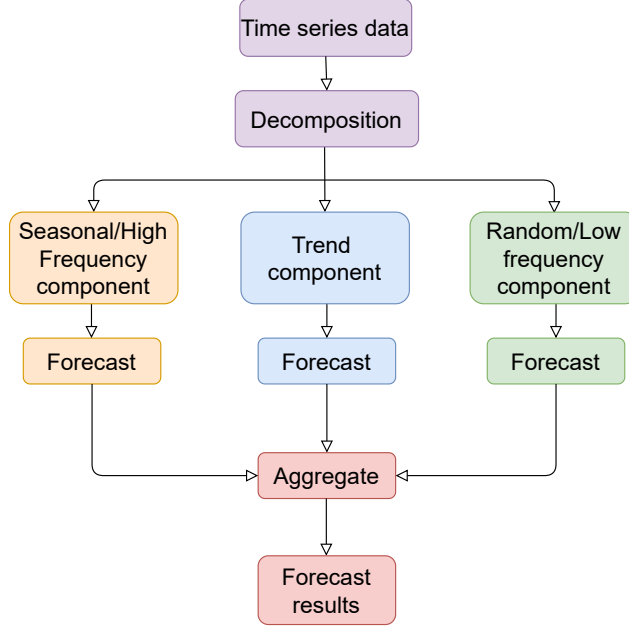


Figure 5: Block diagram of the proposed forecasting methods.

$$\text{MAPE} = \frac{1}{N} \sum_{i=1}^N \frac{|X_i - \hat{X}_i|}{X_i} \times 100\% \quad (7)$$

where X_i and \hat{X}_i are the observed and forecasted data at time t , respectively. N is the number of time steps for forecast evaluation.

Table 2 shows averaged RMSE and MAE values for forecasted 48 values of the time series for seasonal, trend, and random components with the first decomposition approach.

From this table, it concludes that the seasonal component is efficiently predicted with the FFNN model and the other two components with distinct ARIMA models. Similarly, Table 3 shows error values for forecasted 48 values with the second decomposition approach. For all cases, different ARIMA models have fitted accurately and achieved the best forecasting results. In both tables (2 and 3), the last row represents the mean of corresponding time series components.

Table 2: Averaged error values for forecasted 48 values of time series for decomposed components with moving averages with Monte-Carlo strategy for Danish dataset (* indicates best performing method. Both RMSE and MAE are values of CO₂ intensity in gCO₂eq/kWh).

Models	Original time series		Seasonal component		Trend component		Random component	
	RMSE	MAE	RMSE	MAE	RMSE	MAE	RMSE	MAE
ARIMA	44.90	41.92	10.81	09.29	02.79*	02.37*	17.90*	14.70*
FFNN	60.09	55.74	00.03*	00.02*	15.38	14.16	29.38	26.77
PSF	43.92	36.09	01.21	00.59	04.78	03.91	21.45	18.52
DPSF	31.88*	28.46*	09.61	08.66	03.55	03.09	19.92	17.74
Mean	293.1		7.90		82.31		10.88	

3. Performance evaluation of the proposed methods

In this section, the performance and robustness of both decomposition approaches are checked on time series forecasting methods with various distinct trends and seasonality. Then the forecasted results are compared with state-of-the-art methods.

Similar to many other chaotic and intermittent time series found in nature such as wind energy, the CO₂ intensity time series seems to fail at achieving outstanding forecasting performance. These time series are usually infected with unusual and different patterns of trends and seasonality components. Hence, it becomes necessary to choose a method, which can handle trends and seasonality patterns individually to achieve more accurate predictions for such data.

Before the CO₂ intensity data set, the performance of proposed methods based on two mentioned decomposition methods is evaluated for some standard time-series data sets, which are available under a public license. The data sets, used here, are listed in Table 4 and Figure 6. Additionally, the statistical characteristics of the respective time series are provided in Table 5. This table provides the basic statistical details of time series that includes minimum

Table 3: Averaged error values for forecasted 48 values of time series for decomposed components with EEMD method with Monte-Carlo strategy for Danish dataset (* indicates best performing method. Both RMSE and MAE are values of CO2 intensity in gCO2eq/kWh).

Models	Original time series		High-frequency component		Low-frequency component		Trend component	
	RMSE	MAE	RMSE	MAE	RMSE	MAE	RMSE	MAE
ARIMA	44.90	41.92	12.10*	09.07*	01.63*	01.44*	0.005*	0.003*
FFNN	60.09	55.74	13.17	10.08	22.22	19.04	01.99	01.81
PSF	43.92	36.09	15.59	11.32	26.28	25.93	06.33	06.32
DPSF	31.88*	28.46*	23.01	20.80	07.93	06.39	00.05	00.04
Mean	293.1		23.11		27.06		10.03	

(Min.) and maximum (Max.) values, Median, Mean, 1st and 3rd Quartiles.

These time-series data sets were used for performance evaluation of a forecasting model in [29]. The selection of these time series is crucial because special precautions were taken to consider various kinds of seasonality, trend components as well as a variety of periodic and chaotic data sets, which are further discussed in [29]. The amount of chaos in the time series data sets is quantified in terms of the maximum Lyapunov exponent (max. LE) values. The max. LE value of the ‘sunspots’ time series is 0.6009, which makes it a highly chaotic series, whereas, the ‘nottem’ time series is highly periodic with max. LE value of 0.0065. For all of these time series, the last 48 values are taken away for validation purpose, whereas the leftover initial part of the time-series is used for training of the forecasting methods. Then the proposed methods are compared with ARIMA, DPSF, FFNN, and PSF methods. The R package ‘forecast’ [36] is used for ARIMA and FFNN; and ‘PSF’ [37, 38] is used for PSF methods.

Table 6 shows a comparison of the proposed decomposition methods in terms of RMSE values with other methods in the study of a 48-hour forecast. It is observed that the proposed methods achieved better results for almost

Table 4: Details of time series used for validation (Source: [29]).

Time Series	Description
AirPassangers	Time series for monthly totals of international airline passengers for 11 years
nottem	Time series for average air temperature at Nottingham Castle in degree Fahrenheit for 20 years.
sunspots	Time series for monthly mean relative sunspot numbers for more than two centuries.
a10	Total monthly scripts for pharmaceutical products falling under ATC code A10. It is collected by the Australian Health Insurance Commission.
ausbeer	Total quarterly beer production in Australia (in megalitres) reported for more than 50 years.
cafe	Total quarterly expenditure on cafes, restaurants and takeaway food services in Australia collected for around 30 years.
debitcards	Retail debit card usage in Iceland (million ISK).
elecequip	Manufacture of electrical equipment: computer, electronic and optical products.
euretail	Quarterly retail trade index in the Euro area in 17 countries, from 1996 to 2011.
h02	Total monthly scripts for pharmaceutical products falling under ATC code H02, as recorded by the Australian Health Insurance Commission.
usconsumptions	Percentage changes in quarterly personal consumption expenditure and personal disposable income for the US, 1970 to 2010.
usmelec	Electricity net generation measured in billions of kilowatt hours (kWh).

all time-series. Further, the accuracy of the proposed methods is backed by Friedman’s non-parametric test with the distribution of predicted observations. This test is generally used to find differences in treatments within multiple outcomes. Non-parametric means the test does not assume that data belongs to a particular distribution. In this test, the null hypothesis assumes that data comes from a particular distribution. The null hypothesis of this test states that samples in two or more groups are drawn from the same mean value populations. Further, the null hypothesis is rejected when the level of significance is below 0.05.

The p-values for all-time series for Friedman’s test for the proposed methods are shown in Table 7. In all cases, the null hypothesis is rejected with p-values

Table 5: Statistical characteristics of time series used for validation (Source: [29]).

Time Series	Min.	1st Qu.	Median	Mean	3rd Qu.	Max.
AirPassengers	104.0	180.0	265.5	280.3	360.5	622.0
sunspots	0.00	15.70	42.00	51.27	74.92	253.80
nottem	31.30	41.55	47.35	49.04	57.00	66.50
a10	2.815	5.844	9.319	10.694	14.290	29.665
ausbeer	213.0	378.5	423.0	415.0	465.5	599.0
cafe	1012	2190	3389	3716	5193	8426
debitcards	7204	11330	16183	15514	18514	26675
elecequip	62.47	86.17	94.03	95.71	103.95	128.75
eurotail	89.13	94.56	96.55	96.35	99.43	102.10
h02	0.3362	0.5889	0.7471	0.7682	0.9376	1.2572
usconsumptions	-2.2966	0.4050	0.8005	0.7553	1.1141	2.3171
usmelec	139.6	192.6	252.5	254.1	307.0	421.8

lower than 0.05. This concludes that the proposed methods have achieved statistically significant outcomes.

4. CO₂ intensity forecast. A case study

In this section, the performance of the proposed methods is examined for short-term CO₂ intensity forecasting with the consideration of two decomposition approaches. As discussed in earlier sections, these methods are based on two decomposition approaches which decompose a time series into three distinct components. The comparison of these methods is applied for CO₂ intensity forecasting for 48 hours ahead with recursive and Dirrec strategies of predictions. In a recursive approach, the first value is predicted with a prediction model and then appended to the data set. The same model is then used to predict the next value. In the Dirrec approach, the first value is predicted with a model and appended to the data set. A new model is then fitted and used to predict the next value and so on. As the Dirrec approach is a more time-consuming technique, it will be interesting to understand its effect on forecasting accuracy.

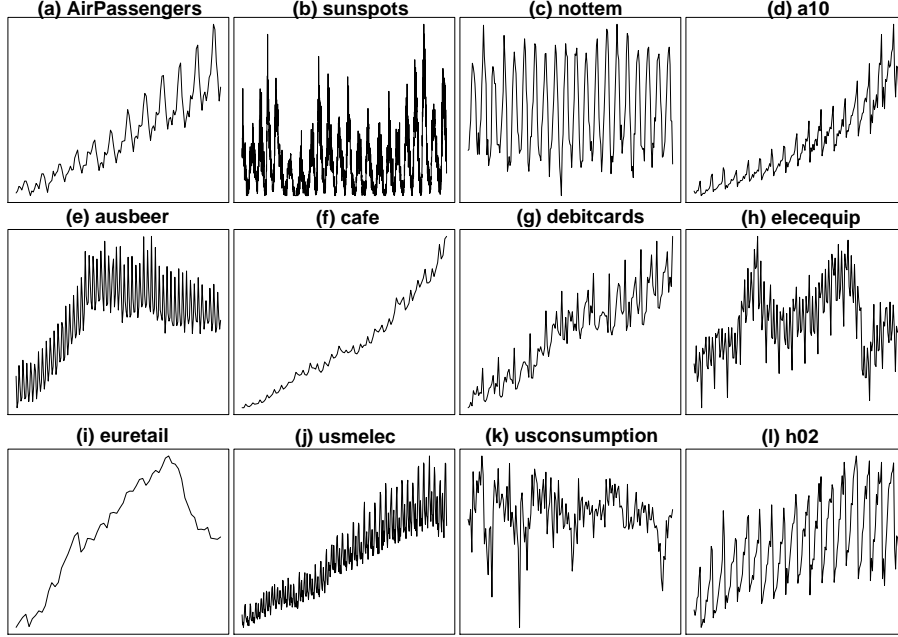


Figure 6: Time series patterns (Source: [29]).

4.1. Data

The data set used in this study is provided by the ENSTO-E Transparency platform [39]. Transmission system operators of each price area report data for production mix, demand, import and export flows, and prices to this platform on daily intervals with hourly resolution. A visualization of this data is provided by the electricityMap [40]. This data for 2017 was the foundation for [16], where a real-time carbon accounting method was proposed for the European electricity markets. This method was based on power flow tracing techniques and introduced a new consumption-based accounting method that represents the underlying physics of the electricity system physics in contrast to the state-of-the-art input-output carbon accounting models [41, 42, 43].

In this case study, data is used from the ENSTO-E Transparency platform for 2018 and 2019. The data set includes electricity generation per technology and electricity demand per price area, as well as power flows between interconnected areas. The flow tracing is used to map power flows between

Table 6: Comparison of proposed methods in terms of RMSE values (* indicates best performing method).

Time Series	ARIMA	FFNN	PSF	DPSF	Method 1	Method 2
AirPassengers	113.72	78.72	97.80	83.09	42.19*	65.31
sunspots	103.07	32.24	52.29	42.51*	47.03	59.34
nottem	2.52	2.46	2.13	2.18	2.01*	2.87
a10	4.88	4.20	6.66	4.65	2.83*	3.18
ausbeer	33.23	33.19	76.85	85.95	30.18*	31.12
cafe	1208.62	2534.18	2888.15	1208.62	1195.02	380.44*
debitcards	2638.13	3353.65	3060.86	6664.44	1029.00*	3069.27
elecequip	27.76	15.80	15.57	32.27	20.79	10.82*
eurotail	06.17	04.52	12.39	08.32	03.13*	05.29
h02	0.22	0.17*	0.08	0.18	0.17*	0.18
usconsumptions	0.98	0.96*	1.15	1.10	0.99	0.99
usmelec	38.33	15.12*	50.22	34.17	21.71	34.27

importing and exporting countries as described in [15]. Country-specific average CO₂ emission intensity per generation technology is applied to the flow tracing results to calculate the hourly CO₂ intensity of electricity consumption for each price area following the method proposed in [16]. It refer to this as the *consumption intensity*. Based on the local generation mix, the CO₂ intensity of electricity generation for each price area is referred to as the *production intensity*.

Figure 7 shows the countries and their inter-connectors (indicating import and export of power flow) for a specific hour considered in the present study. The width of inter-connectors indicates the proportions of the power flow within the countries. And the color allotted to each country represents the consumption-based CO₂ intensity for the specific country within the given color palette. The color sheds vary from green to red color indicating low to high CO₂ intensities for the specific hour.

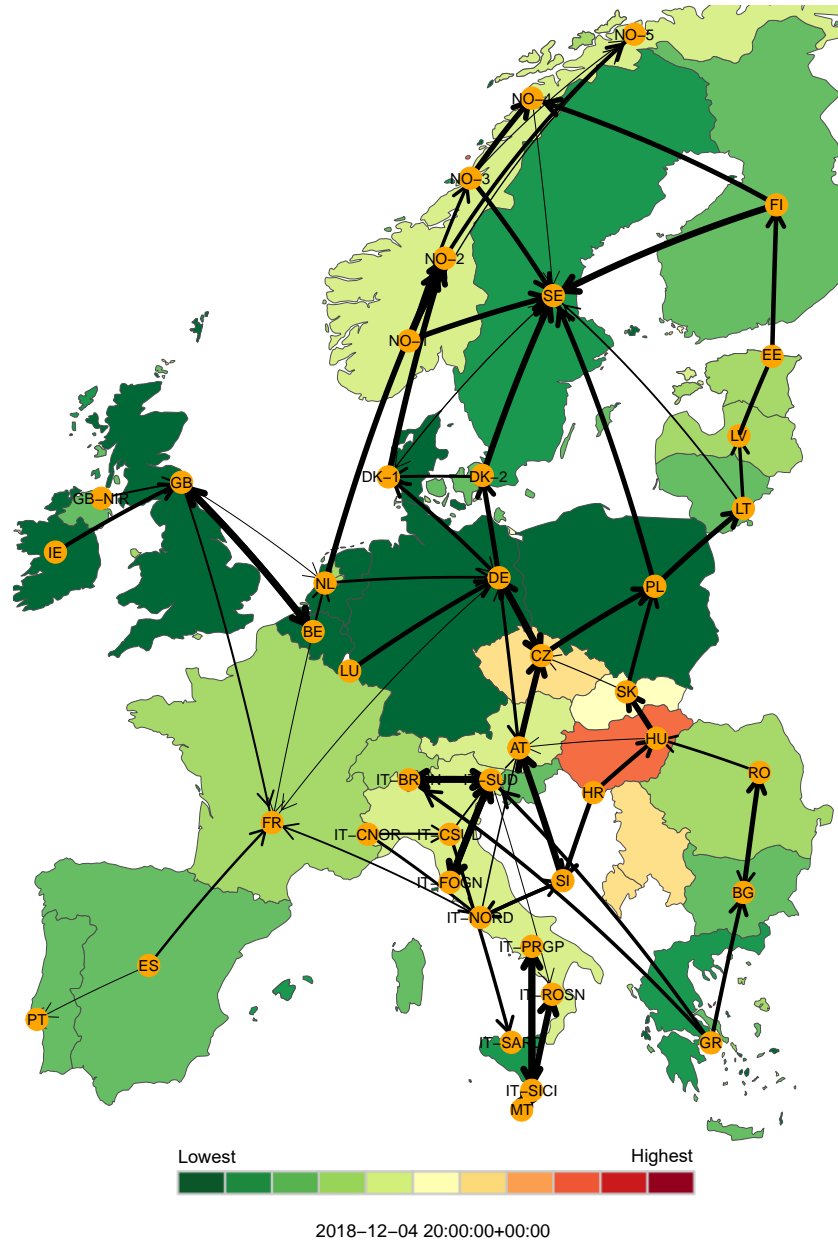


Figure 7: The countries with carbon consumption intensities (shown in different color ranges) and their inter-connectors (indicating import and export of power flow) for a specific hour.

Table 7: p-values of Friedman’s test for proposed methods.

Time Series	Method 1	Method 2
AirPassengers	1.749e-04	2.871e-12
sunspots	7.764e-09	4.262e-12
nottem	2.400e-03	1.222e-12
a10	1.490e-05	1.902e-12
ausbeer	2.141e-10	3.551e-12
cafe	7.764e-09	1.401e-03
debitcards	4.331e-03	4.262e-12
elecequip	7.764e-09	4.002e-12
eurotail	3.147e-11	4.139e-08
h02	4.139e-08	1.974e-12
usconsumptions	1.400e-03	3.892e-03
usmelec	5.312e-05	4.262e-12

In Figure 8, the average hourly production and consumption intensity are compared for each country as a function of the share of non-fossil generation in the country’s generation mix. A clear pattern of decreasing intensity is seen with an increasing share of non-fossil generation. With few exceptions, the consumption intensity is higher than the production intensity for high shares of non-fossil generation. This is an indication of the imported electricity having a higher intensity than the local generation on average. The pattern reverses for low shares of non-fossil generation.

For the detailed demonstration, CO₂ intensity data from 25-05-2019 to 10-07-2019 (i.e. 1248 hours = 52 days) for France is selected randomly for analysis as illustrated in Figure 9. This time series is divided into two parts, i.e., training data which contains data of initial 1200 sampling (1200 hours = 50 days) and validation data as the last 48 samplings (48 hours = 2 days). Further, Table 8 shows the statistical characteristics of the training data set.

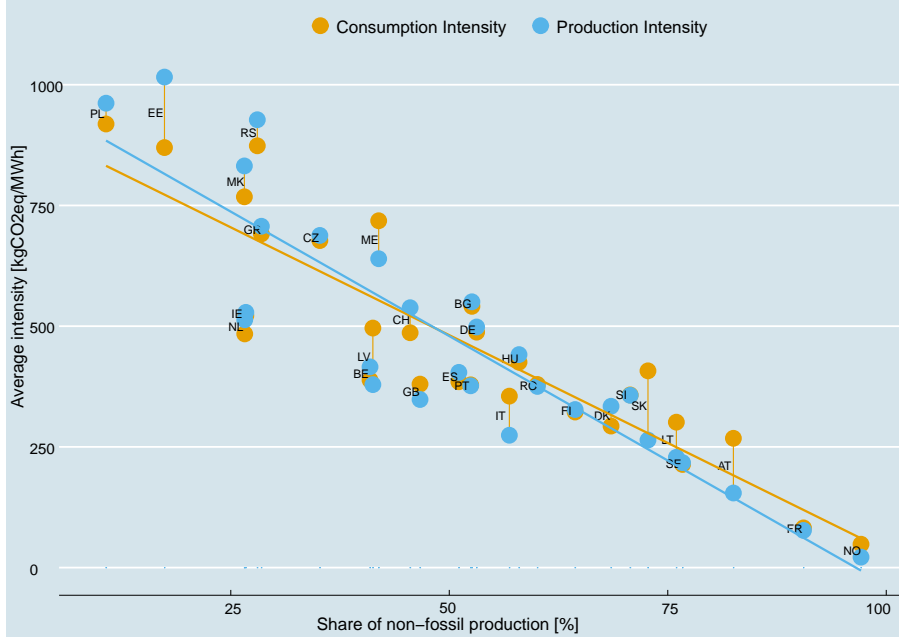


Figure 8: For each country, the compared average hourly production (blue) and consumption (orange) intensity as a function of the share of non-fossil generation in the country’s generation mix.

Table 8: Statistical characteristics of CO₂ intensity time series data set from France.

Location	Mean	Median	Minimum	Maximum	Standard Deviation
France	74.16	78.93	16.35	136.89	27.01

4.2. Model selection

Forecast result accuracy is primarily dependent on the proper selection of models. In this section, the model selection of the proposed methods and state-of-the-art methods are discussed. These state-of-the-art methods are modeled for the original time series as follows. ARIMA models are consist of three parameters, p (number of auto-regressive terms), d (number of nonseasonal differences needed for stationarity) and q (number of lagged forecast errors in the prediction equation); for the given time series these values are 2, 1 and 1, respectively. For PSF models, the optimum window (W) and cluster size

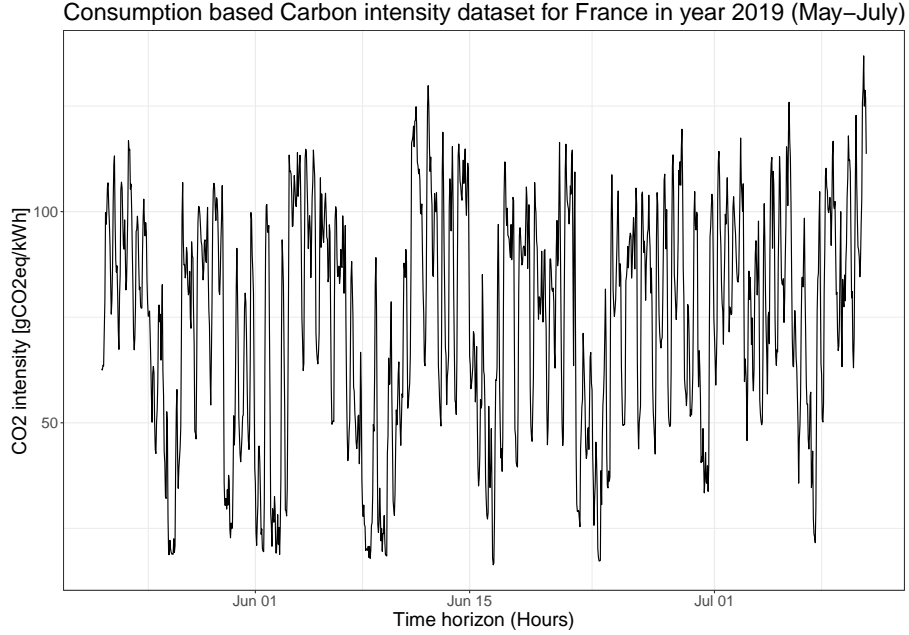
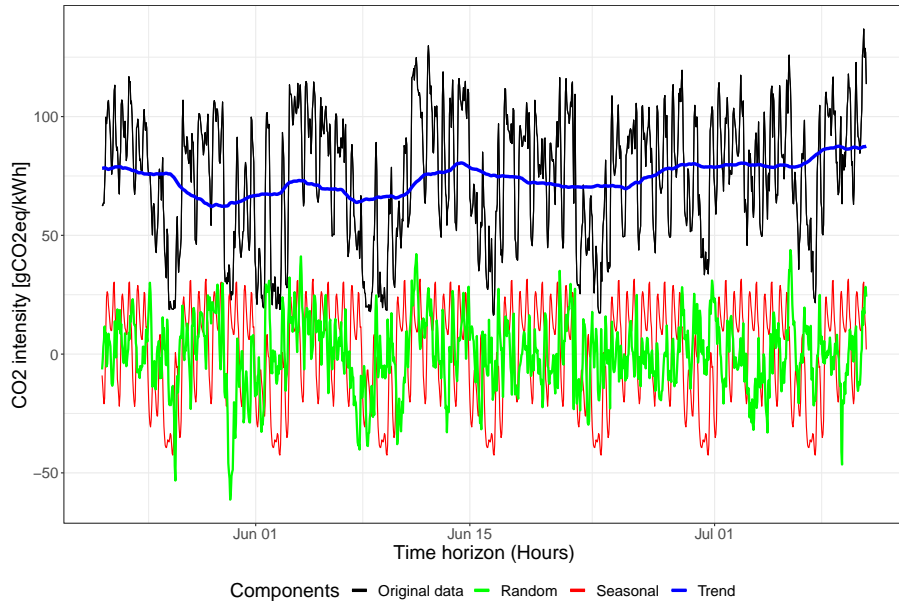


Figure 9: CO₂ intensity time series data set from France for 1248 hours (52 days).

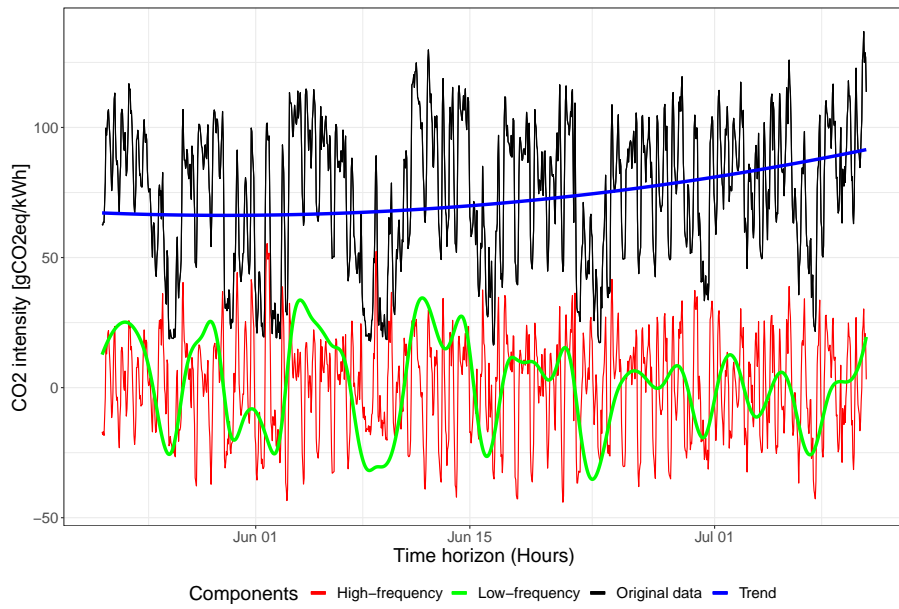
(K) parameters are derived with the R package PSF [38] and for given time series, these values are 4 and 3, respectively. Similarly, for the DPSF model, these values are 5 and 3, respectively. For the FFNN model, two parameters (p lagged inputs and k nodes in the single hidden layer) are calculated and for a given time series, these values are 26 and 14, respectively.

Further, for the first proposed method, there are three models for three components (i.e. seasonal, trend, and random components) and are shown in Figure 10a. For the seasonal component, FFNN is modeled with $p = 28$ and $k = 14$. Whereas, trend and random components are forecasted with ARIMA models. The corresponding parameters are $p = 1$, $d = 1$, $q = 0$ and $p = 3$, $d = 0$, $q = 1$, respectively.

Similarly, in the second proposed method, the time series first decomposes into the number of sub-series with EEMD, named as IMFs. For the given time series, the 10 generated IMFs are shown in Figure 11. Then, with the help of the fine-to-course reconstruction method, all IMFs are combined into three



(a) Decomposition with the moving averages.



(b) Decomposition with EEMD method.

Figure 10: Decomposed components obtained with the (a) moving averages and (b) EEMD method based decomposition approaches.

components based on the mean values of IMFs shown in Figure 12. Then all three components (i.e. low-frequency, high-frequency, and trend components) shown in Figure 10b are forecasted with ARIMA models with parameters as shown in Table 9.

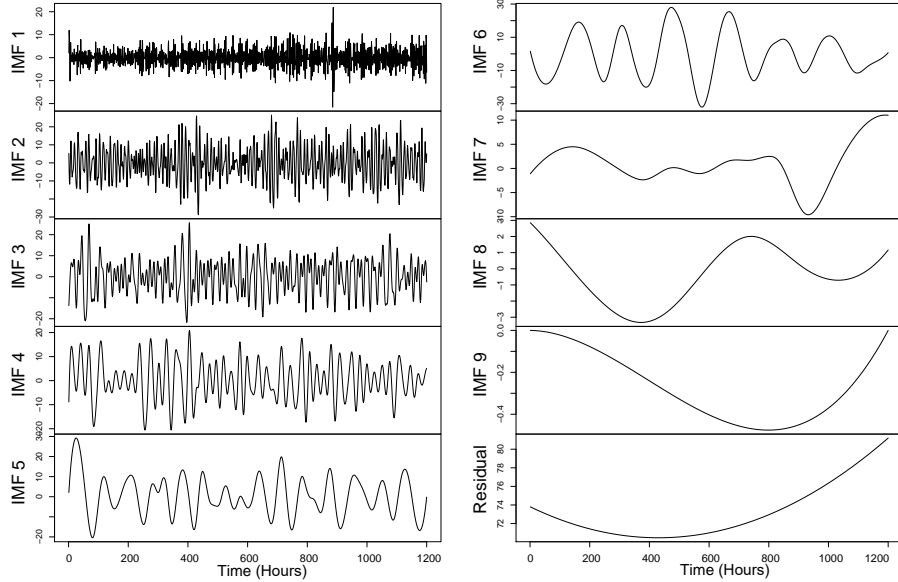


Figure 11: Decomposition of CO₂ intensity [gCO₂eq/kWh] time series for France.

Table 9: Parameters for ARIMA models in Method 2.

Components	Models	p	d	q
High-frequency	ARIMA	2	0	3
Low-frequency	ARIMA	1	0	0
Trend	ARIMA	0	2	0

4.3. Results and discussion

This subsection discusses the forecasting results of both proposed methods on the CO₂ intensity time series data set from several European countries. Apart from the comparison of both decomposition-based methods, other state-of-the-art forecasting methods have been compared in the study to prove the

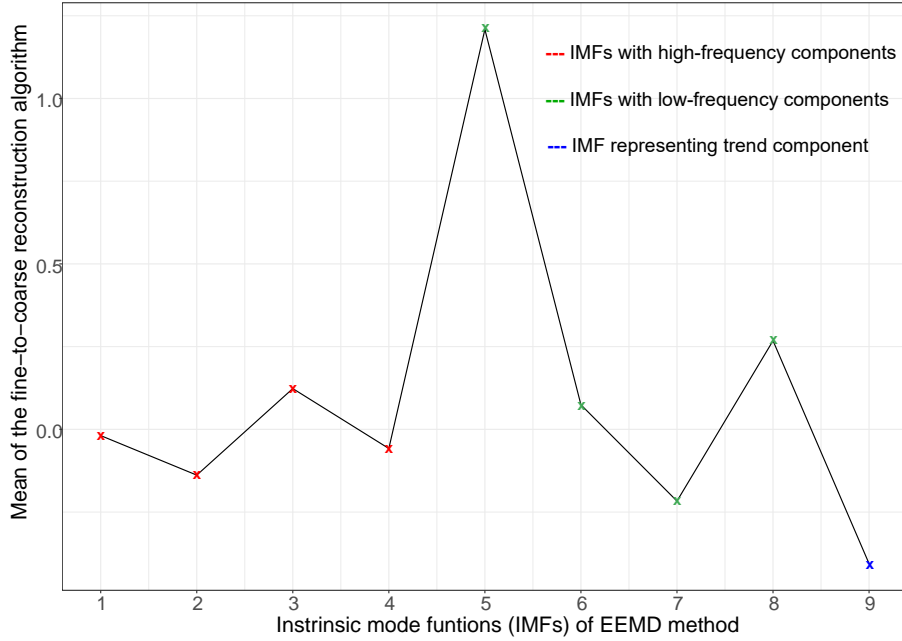


Figure 12: The mean of the fine-to-coarse reconstruction algorithm as a function of index K .

accuracies of both strategies. These models include ARIMA, FFNN, SVM, PSF, and DPSF, which are among the best ones to perform on such chaotic and intermittent data set used in this study. All these models are compared with both recursive and Dirrec prediction approaches for 48 hours ahead forecasting results for the French data set and are shown in Table 10. For both approaches, the proposed models show better forecasting performance in terms of RMSE, MAE, and MAPE with Method 1 outperforming Method 2. There are several models to forecast one or two-step ahead values precisely.

Furthermore, all these models are examined for the same French data set for different multi-step ahead forecasting. Figure 13 shows the error values (RMSE) with distinct models for 1, 3, 6, 12, 24 and 48 hours ahead forecasts. It can be seen that concerning the proposed methods, ARIMA, PSF, and DPSF models are showing lower or comparable errors for shorter multi-step forecasts, but it gets drastically higher for longer steps (48-step ahead) ones. Whereas,

Table 10: Comparison of proposed methods with state-of-the-art models for CO₂ intensity data in France (* indicates the best performing method).

Models	Recursive approach			Dirrec approach		
	RMSE	MAE	MAPE	RMSE	MAE	MAPE
ARIMA	28.86	22.83	21.64	28.34	22.41	21.40
FFNN	26.43	20.28	21.14	25.93	19.73	20.88
SVM	62.96	50.50	59.20	58.11	43.90	55.05
PSF	20.47	15.31	15.26	20.38	15.29	15.21
DPSF	26.12	21.93	22.62	26.05	21.88	22.56
Method 1	15.57*	11.99*	11.47*	15.53*	11.80*	11.46*
Method 2	18.28	14.58	15.98	18.16	14.43	15.91

for 48 hours ahead forecast, both proposed models have shown higher accuracy, and especially Method 1.

Apart from this, the statistical significance of the proposed methods is evaluated with Friedman’s test. The p-values of this test for the French data set are 0.020 and 0.057 for the 48 hours ahead forecast for Method 1 and Method 2, respectively. In both cases, the null hypothesis is rejected with lower p-values and approves its statistical significance.

In such studies, the complexity of a methodology is considered as an important metric apart from forecasting error comparison to evaluate the forecasting performance. Usually, the complexity is estimated only with the size of the data set, not other possible parameters such as the number of features, tuning parameters, etc. In the present study, the time complexity of the proposed methods is estimated with the GuessComp tool [44]. This tool empirically guesses the time and memory complexities of a methodology. It tests multiple, increasing size random samples of the input data sets and attempts to fit distinct complexity function $O(N)$, $O(N^2)$, $O(\log N)$, etc. Based on the best fit, this tool estimates the full computational time for given data set and it is discussed in detail in [45].

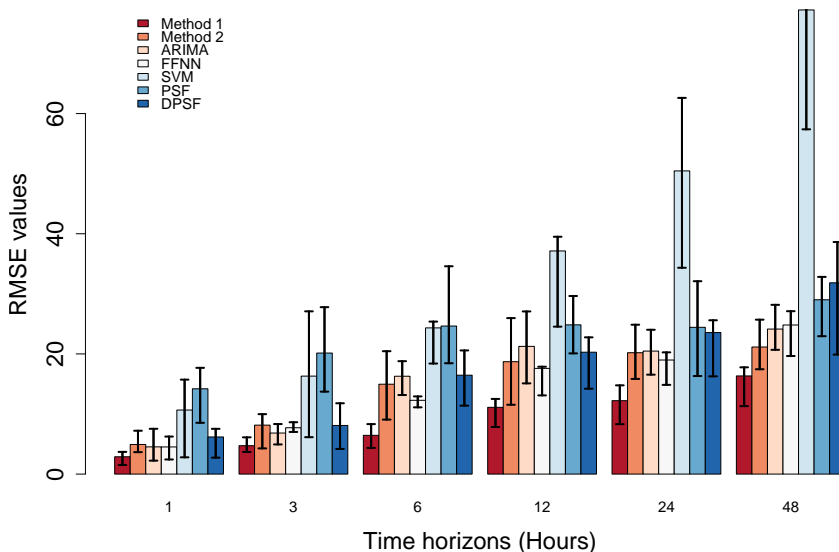


Figure 13: Multi-step ahead error values (RMSE) with various models for France.

Table A.1 shows the time and memory complexities of individual decomposition approaches and forecasting models for each decomposed component for both proposed methods for the French data set. The overall complexities of both methods are calculated by observing the complexities of each sub-step involved in the methods. This individual complexity study is done since all sub-steps (decomposition and forecasting models) are performed on different data series.

The overall complexity of the methods is finalized based on the most complex process within each method. In Method 1, the seasonal component forecasting with the FFNN model is the most complex step with quadratic ($O(N^2)$) nature in terms of time complexity. Hence, the overall time complexity of Method 1 is quadratic ($O(N^2)$). Similarly, the decomposition approach in Method 2 appeared to be the most time consumption-based complex task, which is Linearithmic $O(N \log N)$. Furthermore, the memory complexity is observed to be the Logarithmic $O(\log N)$ for both methods. Considering the

same length of time series, similar complexity observations are obtained for the other countries.

An unbiased comparison study is performed with the Monte-Carlo strategy for all countries', in which 25 different patches of 1248 continuous samples are selected randomly. For each patch, initial 1200 samples are used as training data and the remaining 48 values are used for validation purposes. Finally, the mean of error values for each patch is considered as the performance of the methods compared in the study. This Monte-Carlo strategy is implemented with the ForecastTB tool [46, 47], and it ensures the suitability of the models for the given time series and rejects the possibility of favorable results by chance.

Based on Tables 10, 11, and A.1, the following points can be observed:

- For the sample French data set, both proposed methods have performed better than other models for 48 hours ahead CO₂ intensity forecasting. The RMSE, MAE, and MAPE of Method 1 are 15.57, 11.99, and 11.47 for the recursive approach; and 15.53, 11.80, and 11.46 for Dirrec one. Whereas, in Method 2, for the recursive approach, these errors are 18.28, 14.58, and 15.98; and for the Dirrec approach are 18.16, 14.43, and 15.91, respectively. In terms of RMSE, Method 1 has 14.82% and 14.48% improvement in forecasting in comparison to Method 2 for recursive and Dirrec approaches.

The percentage of improvements with Method 1 as compared to all other methods in the study are shown in Table 12 for both recursive and Dirrec approaches.

- Dirrec is found to be an expensive forecasting strategy in which the first forecasted value is appended to the data set and a new model is fitted to forecast the next value. It means, for 48 hours ahead forecast, the execution time of the Dirrec model is nearly 48 times that of the recursive one. From Tables 10 and 12, it can be seen that the error improvements with Dirrec strategy are negligible as compared to the recursive one. Hence,

Table 11: Comparison of proposed methods with state-of-the-art models in terms of RMSE for CO₂ emissions data for European countries (* indicates the best performing method for the respective country).

Country	ARIMA	FFNN	SVM	PSF	DPSF	Method 1	Method 2
Austria	52.42	50.93	51.66	57.20	51.82	35.49*	46.34
Belgium	191.75	200.17	298.35	223.17	321.50	195.17	181.22*
Bulgaria	36.40	55.15	85.12	61.21	43.14	32.98	31.71*
Switzerland	95.52	96.33	62.63	95.60	139.56	86.04*	95.00
Czech Republic	71.33	74.49	87.92	86.08	74.94	49.01*	63.91
Germany	102.72	85.70	106.71	83.40	77.96	42.18*	62.77
Denmark	30.74	40.65	84.52	42.49	46.11	31.09	28.09*
Estonia	87.48	122.11	244.91	100.38	117.31	57.70*	64.45
Spain	132.35	134.81	126.32	147.66	226.93	131.89*	135.57
Finland	21.31	39.76	45.30	23.88	28.00	18.00	16.57*
France	22.80	26.10	52.86	21.44	22.35	14.91*	20.49
UK	149.87	332.34	298.71	171.00	176.16	140.35	133.75*
Greece	72.11	48.01	96.65	46.72	35.61	30.68*	43.69
Hungary	29.69	45.54	61.60	45.84	29.52	16.13*	26.50
Ireland	71.46	70.47	95.88	68.17	63.39	45.23*	67.66
Italy	120.33	120.51	152.04	85.24	80.58	48.66*	111.43
Lithuania	86.81	122.01	213.56	78.77	98.17	61.59*	76.44
Latvia	66.62	79.01	89.68	62.05	83.67	49.11*	56.59
Montenegro	166.84	170.73	234.48	132.44	161.84	97.44*	151.89
North Macedonia	74.44	65.44	89.26	82.73	92.14	67.37	58.81*
Netherlands	53.99	84.66	52.94	56.57	55.30	43.27*	44.11
Norway	59.36	81.32	167.89	69.09	57.32	37.70*	42.38
Poland	64.03	68.62	85.79	62.75	51.59	50.30*	52.09
Portugal	56.50	56.74	80.74	66.73	61.95	48.90*	53.75
Romania	37.06	43.55	47.62	51.20	43.31	33.02*	36.96
Serbia	57.00	42.77	96.06	71.87	85.83	44.44*	51.72
Sweden	67.97*	108.96	102.01	71.79	59.68	69.59	74.19
Slovenia	45.96	40.63	59.83	53.34	40.37	29.23*	31.55
Slovakia	34.92	36.84	60.47	43.46	42.73	27.90*	33.69

Table 12: Percentage improvements of Method 1 with state-of-the-art models for CO₂ intensity data in France.

Models	Recursive approach			Dirrec approach		
	RMSE	MAE	MAPE	RMSE	MAE	MAPE
ARIMA	46.04	47.48	46.99	45.20	47.34	46.44
FFNN	41.08	40.82	45.74	40.10	40.19	45.11
SVM	75.52	76.23	80.62	73.23	73.12	79.18
PSF	23.93	21.61	24.83	23.79	22.82	24.65
DPSF	40.39	54.28	49.29	40.38	46.06	49.20
Method 2	14.82	17.69	28.22	14.48	18.22	27.96

the recursive strategy comes out to be the better-suited forecasting strategy for short-term multi-step CO₂ intensity forecasting.

- Based on Table 11, with the Monte-Carlo strategy, among 29 European countries, Method 1 outperformed all methods for 22 countries, and for 6 countries, Method 2 was the best performing method. The overall average percentage improvements of Method 1 as compared to ARIMA and FFNN methods range from -2.38% (for Sweden) to 58.93% (for Germany) and -3.97% (for Serbia) to 64.58% (for Hungary), respectively in terms of RMSE collectively for all countries. Similarly, the same improvements ranges with Method 2 are -9.15% (for Sweden) to 39.41% (for Greece) and -20.92% (for Serbia) to 59.74% (for UK), respectively. Here, the negative sign indicates that Method 1 or 2 performed in a less efficient way than the methods in the comparison study. The country-wise percentage improvements in RMSE for ARIMA and FFNN methods are shown in Figures 14 and 15, respectively.
- Method 1 achieved superior accuracy with the statistical significance at the cost of computational complexity. Considering the computational complexity (especially, the time complexity), Method 1 ($O(N^2)$) observed

more complex than Method 2 ($O(N \log N)$).

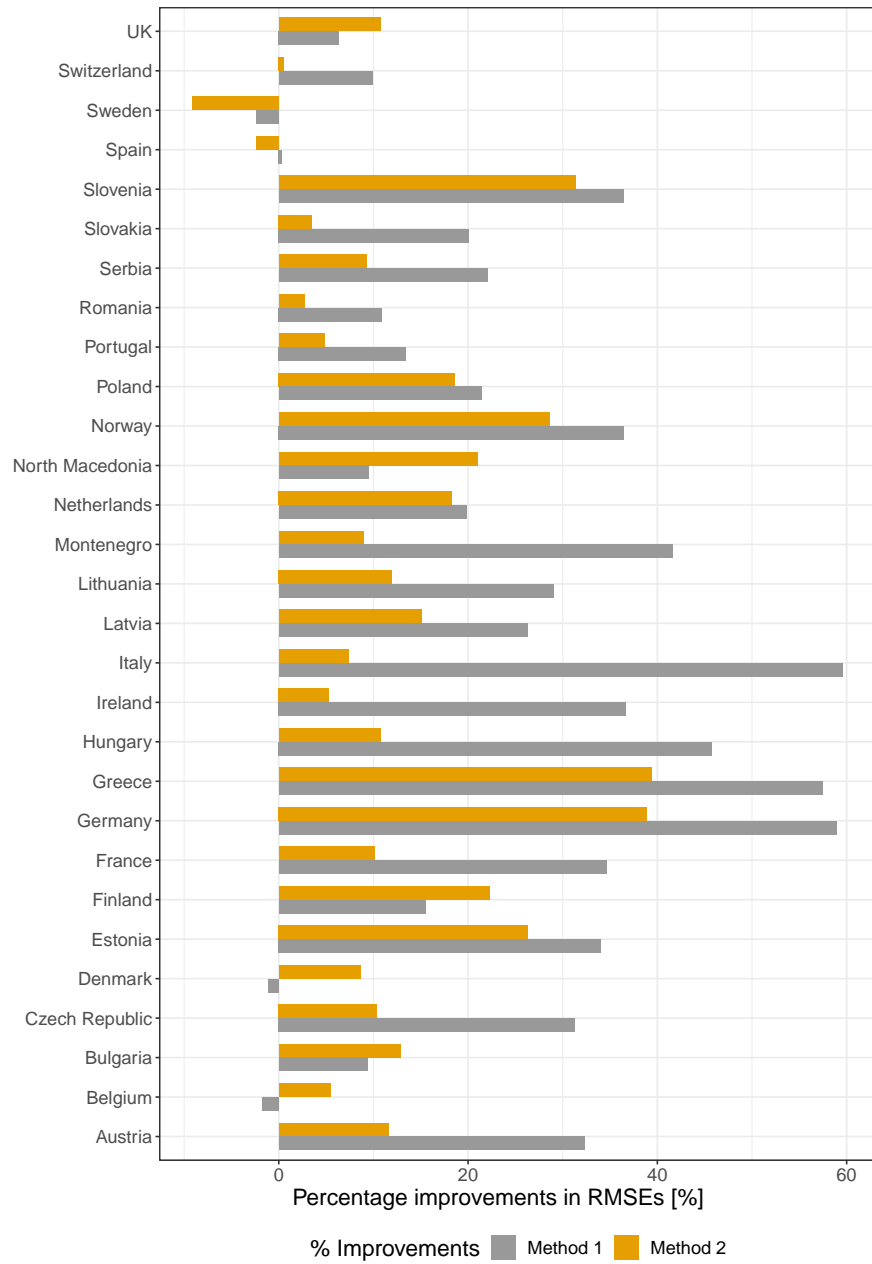


Figure 14: Percentage improvements in RMSE with respect to ARIMA.

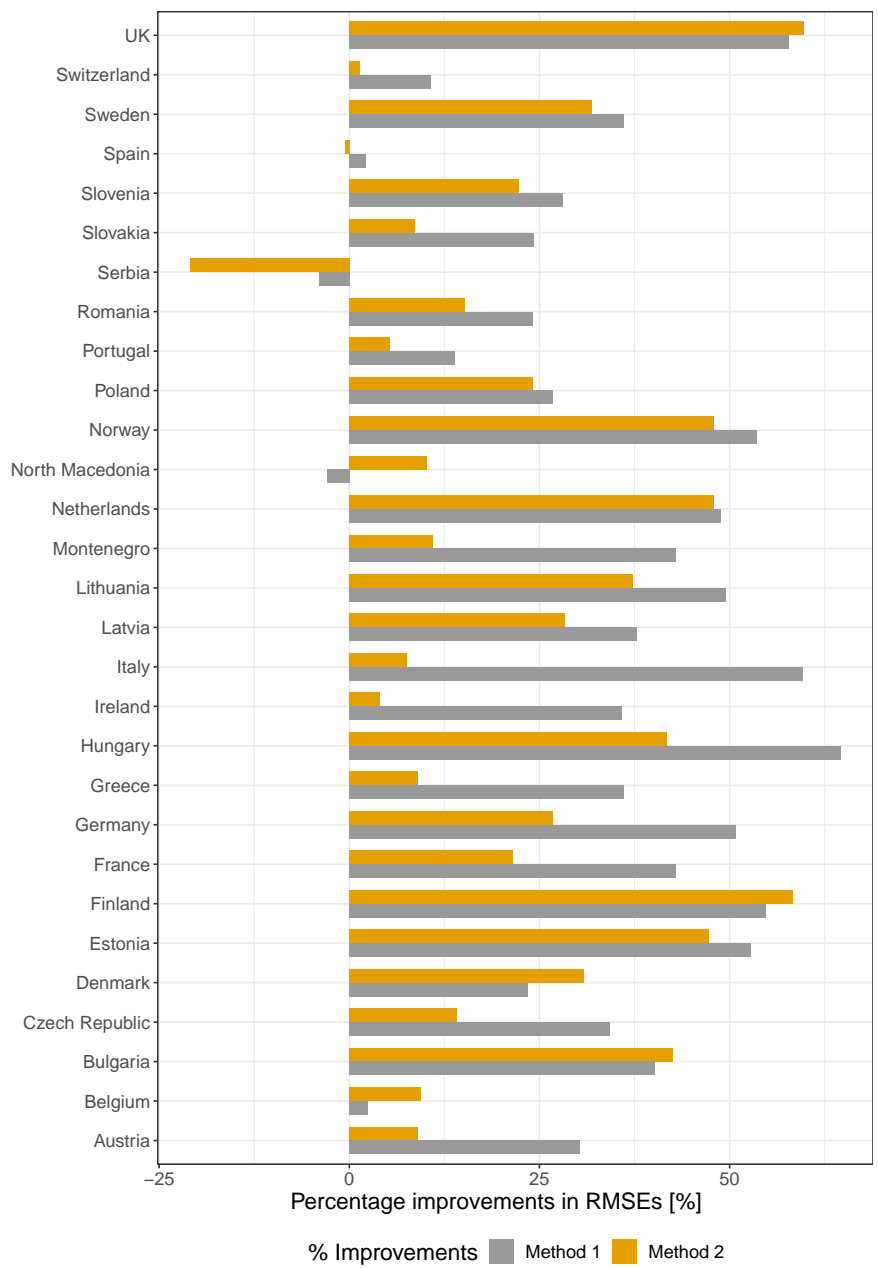


Figure 15: Percentage improvements in RMSE with respect to FFNN.

5. Impact on electricity market scheduling

The ultimate goal of the short-term CO₂ intensity forecast is to enable the scheduling of flexible demand in the electricity market to minimize the resulting CO₂ emissions. Figure 16 shows the realized CO₂ emissions per kWh electricity consumed (black) and corresponding forecasted values (red) with Method 1 for France for consecutive 48 hours. The start point of the time series (12.00 PM) is the point in time today (day D) at which the day-ahead electricity market is cleared. Bids submitted to the day-ahead power exchange before this time is targeted the whole of the next-coming day (24 hours of the day $D + 1$). This interval is marked in the grey between the dashed blue lines.

In this example, a flexible electricity consumer is willing to bid in specific hours in day $D + 1$ to minimize the associated CO₂ emissions. Specifically, electricity consumption is scheduled during the four hours with least forecasted CO₂ intensity. The dots on the red line denote the four minimum values of the forecast within the 24-hour window. The horizontal line shows the maximum CO₂ emissions per kilowatt-hour electricity consumed value within the scheduled hours with reference to the forecasted series. The dots on the black line highlight the corresponding realized values. The mean intensity for these four hours is 76.35 gCO₂eq/kWh and 72.51 gCO₂eq/kWh, respectively, for the forecasted and realized values.

Similar examples of scheduling for Germany, Norway, Denmark, and Poland are shown in Figure B.1. These countries have been selected based on their location in Figure 8: Poland with a very low share of non-fossil generation, France with a high share of nuclear, Norway with a high share of hydro, Denmark with a high share of wind and Germany somewhere in between.

Figure 16 shows just a single example of scheduling four hours of electricity consumption in France. In Figure 17, the emissions between scheduling and consuming are compared at a random time during the 24-hour interval for an entire year in France. Each bar shows results for different durations of flexible consumption from one to 24 hours. The ratio between the bars is shown as the

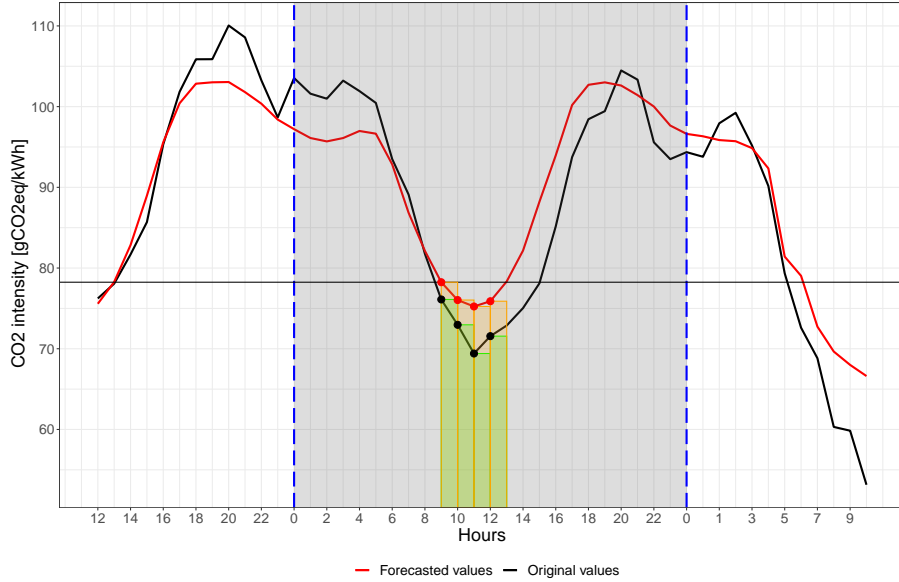


Figure 16: Example of scheduling 4 hours of flexible electricity consumption one day in advance in France. The gray area shows the day-ahead interval. The red and black lines show forecasted and realized values of the CO₂ intensity, respectively. The four hours minimum of the forecast is market with red dots. The corresponding realized values are marked with black dots.

red line. A ratio of one means there are no savings from scheduling compared to consuming at a random time. This is the case when the flexible consumption takes up all 24 hours of the window. The ratio decreases as the duration of flexible consumption decreases. This is to be expected as a shorter duration of consumption means more flexibility for scheduling during the 24 windows.

Figure 18 shows similar results for Germany, Norway, Denmark, and Poland. Comparing the benefit of scheduling between the five countries, for a duration of flexible consumption of four hours, observed on average 25 % emissions reductions in France, 17 % in Germany, 69 % in Norway, 20 % in Denmark, and just 3 % in Poland.

Furthermore, Figure 19 shows the variation in the ratio of forecasted (V_F) and realized (V_V) values for each of the 48 hours of the forecast horizon with

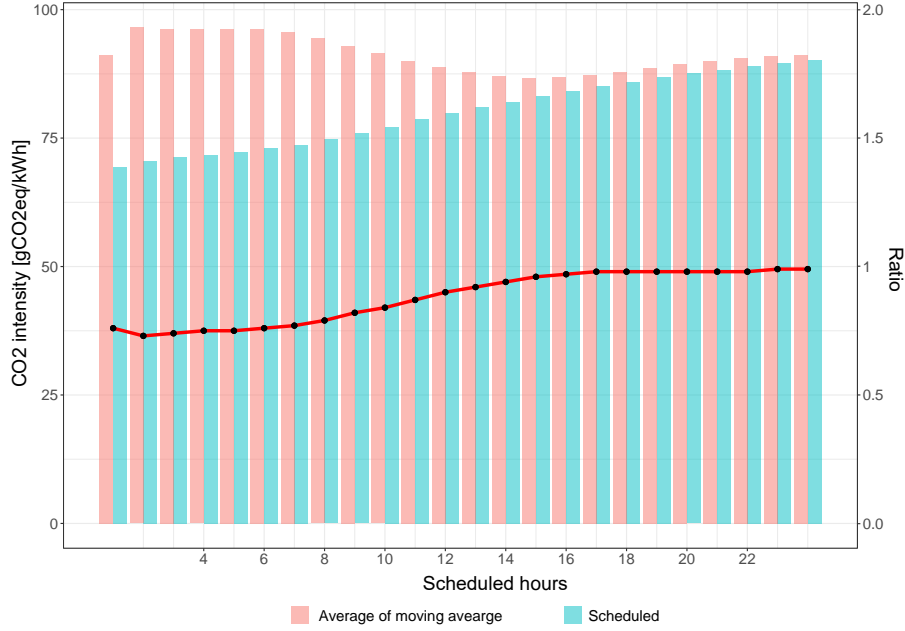


Figure 17: Comparison of emissions between scheduling and consuming at a random time during the 24-hour interval for an entire year in France. Each bar shows results for different durations of flexible consumption. The ratio between the bars is shown as the red line.

Monte-Carlo strategy with 50 iterations for France. This figure represents the statistical relation between forecasted and realized values in terms of box plots. The red dots are the mean values of these ratios for the whole year. The dashed blue lines show the standard deviations from the mean values throughout the year. The shaded regions in the figure show the 24 hours of the forecasts, which are to be used for the scheduling of flexible consumption. It is observed that the forecast at initial and last 8 hours is more consistent throughout the year, whereas, those in middle hours (day-time hours) express higher variations. This outcome concludes that, though these variations are not much significant (merely varies between 0.091 to 0.185) throughout the year, the electricity market bidder could consider a bit higher chances of deviation in the day time hour values. Similar results for Denmark, Germany, Norway, and Poland are shown in Figure B.2.

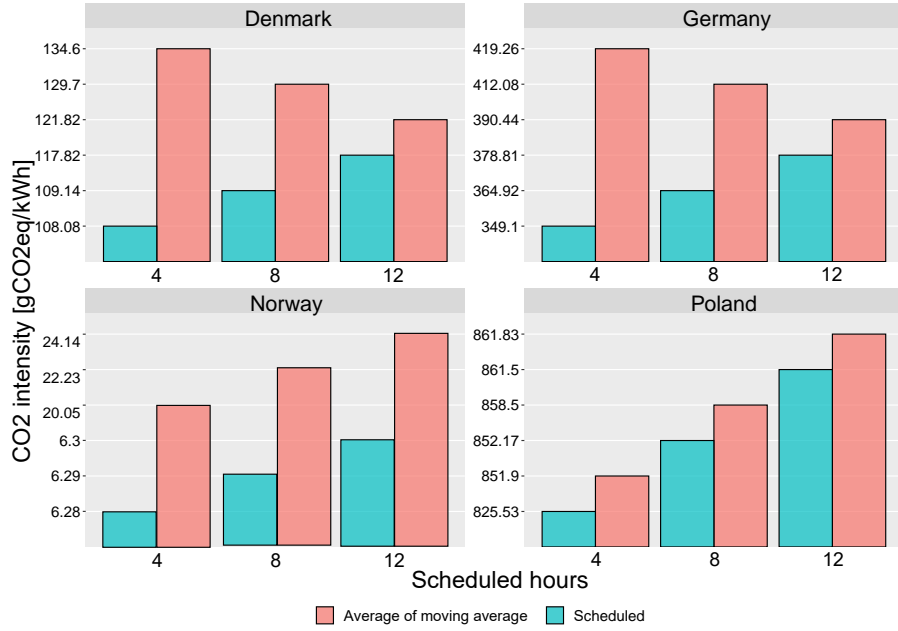


Figure 18: Comparison of emissions between scheduling and consuming at a random time during the 24-hour interval for an entire year in four countries. The bars show results for durations of flexible consumption of 4, 8 and 12 hours.

6. Conclusions

Accurately forecasting the CO₂ intensity plays a crucial role in the socio-economic and environmental benefits derived from appropriate energy management. It can affect the energy policies of a country to a certain extent. Hence, more accurate methods to improve CO₂ intensity forecasts become sensible. A simple model without preprocessing of a chaotic time series usually seems unachievable in most of the cases. Hence, the preprocessing of the data set with suitable methodologies enhances the forecasting accuracy. Preprocessing with decomposition methods helped many researchers in superior forecasting outcomes.

In this study, the accuracies of two decomposition strategies are examined for 48 hours ahead of CO₂ intensity data forecasting. The first decomposition approach is a pure and simple statistical method that decomposes a time

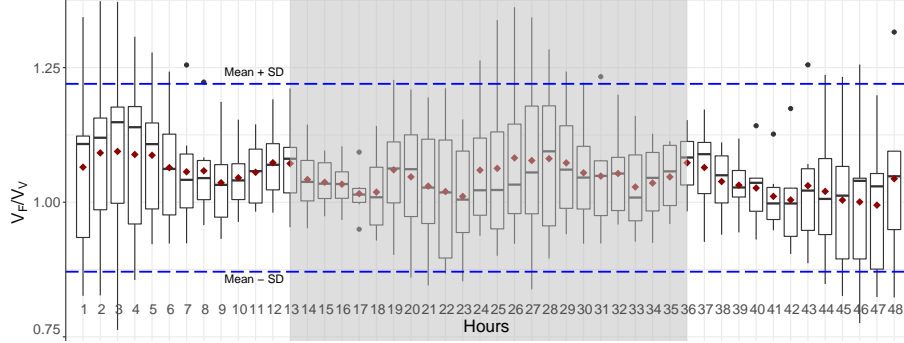


Figure 19: Variation in the ratio of forecasted (V_F) and realized (V_V) values for each of the 48 hours of the forecast horizon. The red dots in are the mean values of these ratios for the whole year. The dashed blue lines show the standard deviations from the mean values throughout the year. The shaded regions show the 24 hours of the forecasts, which are to be used for the scheduling of flexible consumption.

series into seasonal, trend, and random series components. Similarly, the second decomposition approach bases on the EEMD method again decomposes a time series into three components, those are, high-frequency, low-frequency, and trend series components. These decomposition approaches separate out of distinct meaningful patterns from the original time series and assists in achieving forecast-friendly data series components. Summarizing the observation, it can be concluded that the performance of meaningful decomposition approaches can improve the multi-step short-term CO_2 intensity forecast as discussed in the paper. In this study, for CO_2 intensity forecasting, the first decomposition-based method (with time complexity $O(N^2)$) has been found to outperform the second method with time complexity $O(N \log N)$). For 23 of the 29 European countries, the first decomposition method obtained the highest accuracy. The result is a trade-off between forecast accuracy and computational complexity. The memory complexity of both methods is the same, i.e., $O(\log N)$. In this case, the higher computing time is acceptable since the forecast is only performed once per day for the day-ahead market.

After validating the correctness of Method 1 of the proposed forecasting method, it was used to assess the impact scheduling of flexible electricity

consumption. The CO₂ emissions from scheduling were studied for France, Germany, Norway, Denmark, and Poland. It was found for all countries that scheduling the consumption after the forecasted intensity compared with consuming at a random time leads to reductions in emissions. Reductions increase with decreasing duration of consumption because of the increased flexibility of scheduling within the 24-hour window. In the case of a duration of flexible consumption of four hours, it found emissions reductions ranging from 3 % in Poland to 69 % in Norway.

In future work, forecasts with a longer horizon and finding the optimal trade-off between CO₂ emissions and electricity prices can be examined to propose a meaningful strategy for scheduling flexible electricity consumption in the day-ahead and future markets of electricity.

Acknowledgments

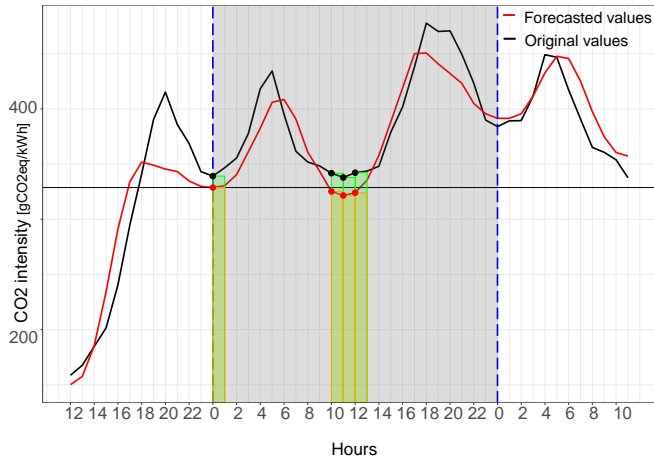
This study was funded by Apple Inc. as part of the APPLAUSE bio-energy collaboration with Aarhus University. Bo Tranberg acknowledges funding from ELFORSK via project 351-054.

A. Tables

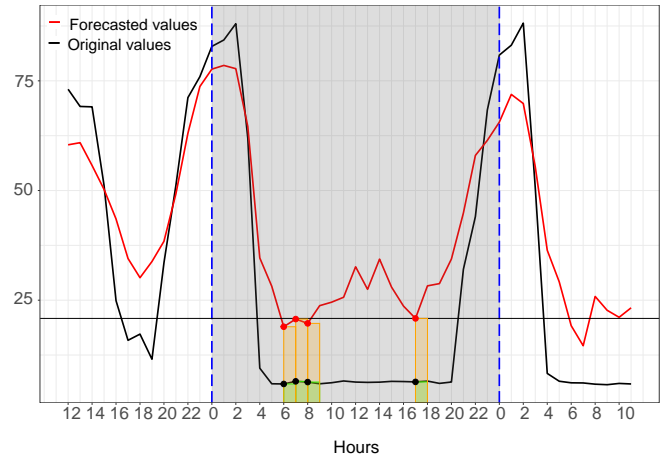
Table A.1: Complexity study of the proposed methods.

Complexity of Method 1					
Complexity	Decomposition with moving averages	Seasonal component forecast with FFNN	Random component forecast with ARIMA	Trend component forecast with ARIMA	Overall
Time	Constant $O(1)$	Quadratic $O(N^2)$	Constant $O(1)$	Logarithmic $O(\log N)$	Quadratic $O(N^2)$
Memory	Logarithmic $O(\log N)$	Constant $O(1)$	Logarithmic $O(\log N)$	Logarithmic $O(\log N)$	Logarithmic $O(\log N)$
Complexity of Method 2					
Complexity	Decomposition with EEMD method	High-freq. component forecast with ARIMA	Low-freq. component forecast with ARIMA	Trend component forecast with ARIMA	Overall
Time	Linearithmic $O(N \log N)$	Constant $O(1)$	Constant $O(1)$	Constant $O(1)$	Linearithmic $O(N \log N)$
Memory	Logarithmic $O(\log N)$	Constant $O(1)$	Constant $O(1)$	Logarithmic $O(\log N)$	Logarithmic $O(\log N)$

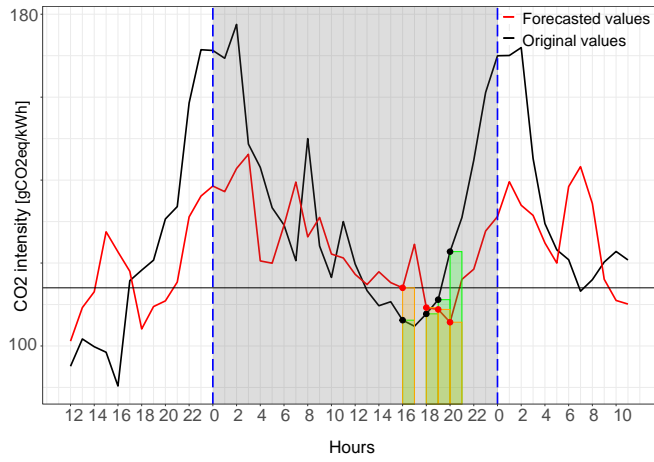
B. Figures



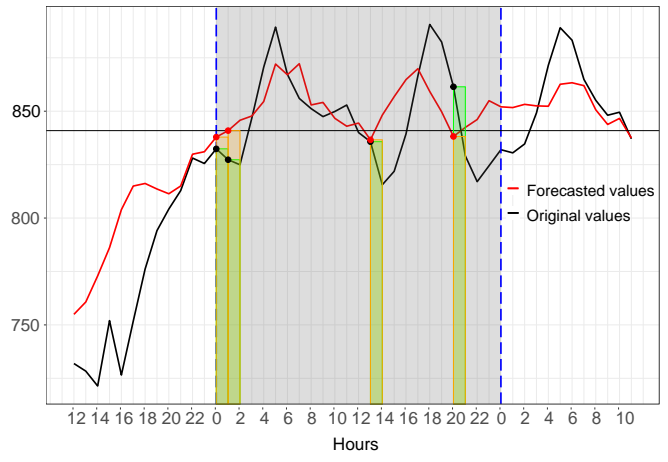
(a) Germany



(b) Norway



(c) Denmark



(d) Poland

Figure B.1: Example of scheduling 4 hours of flexible electricity consumption one day in advance in four different countries. The gray area shows the day-ahead interval. The red and black lines show forecasted and realized values of the CO₂ intensity, respectively. The four hours minimum of the forecast is marked with red dots. The corresponding realized values are marked with black dots.

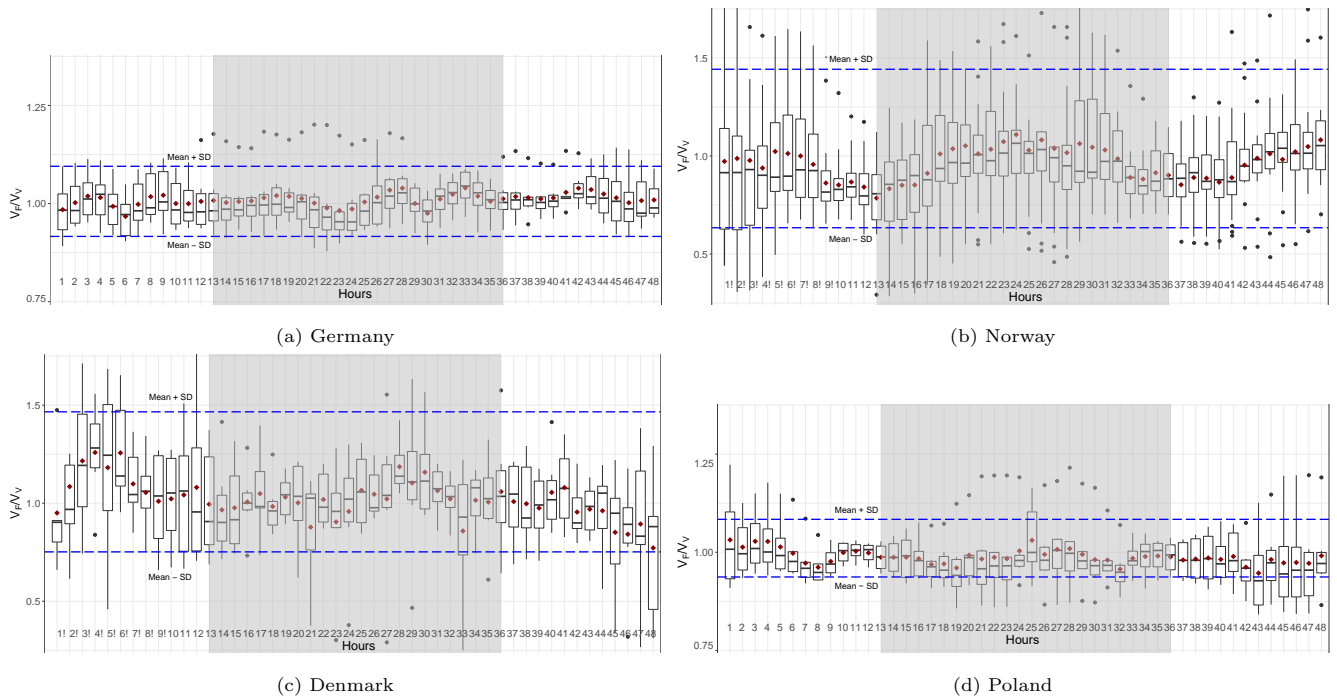


Figure B.2: Variation in the ratio of forecasted (V_F) and realized (V_V) values for each of the 48 hours of the forecast horizon. The red dots in are the mean values of these ratios for the whole year. The dashed blue lines show the standard deviations from the mean values throughout the year. The shaded regions show the 24 hours of the forecasts, which are to be used for the scheduling of flexible consumption.

References

References

- [1] IPCC, Special Report: Global Warming of 1.5°C (2018).
- [2] T. Ming, S. Caillol, W. Liu, et al., Fighting global warming by GHG removal: Destroying CFCs and HCFCs in solar-wind power plant hybrids producing renewable energy with no-intermittency, *International Journal of Greenhouse Gas Control* 49 (2016) 449–472.
- [3] European Commission, Fossil CO₂ emissions of all world countries - 2018 Report. doi:10.2760/30158.
- [4] International Energy Agency, Data & Statistics, <https://www.iea.org/data-and-statistics>, accessed: 2020-07-23.
- [5] Wikipedia - 2009 united nations climate change conference, https://en.wikipedia.org/wiki/2009_United_Nations_Climate_Change_Conference, accessed: 2019-12-31.
- [6] W. Chen, F. Wu, W. Geng, G. Yu, Carbon emissions in china's industrial sectors, *Resources, Conservation and Recycling* 117 (2017) 264–273.
- [7] The Paris Agreement, <https://unfccc.int/process-and-meetings/the-paris-agreement/the-paris-agreement>, accessed: 2019-12-31.
- [8] Carbonbrief, <https://www.carbonbrief.org/>, accessed: 2019-12-31.
- [9] F. Ye, X. Xie, L. Zhang, X. Hu, An improved grey model and scenario analysis for carbon intensity forecasting in the pearl river delta region of china, *Energies* 11 (1) (2018) 91.
- [10] L. Zhou, X. Zhang, T. Qi, J. He, X. Luo, Regional disaggregation of china's national carbon intensity reduction target by reduction pathway analysis, *Energy for Sustainable Development* 23 (2014) 25–31.

- [11] K. Chang, H. Chang, Cutting CO₂ intensity targets of interprovincial emissions trading in China, *Applied Energy* 163 (2016) 211–221.
- [12] Nord Pool, <https://www.nordpoolgroup.com>, accessed: 2019-12-31.
- [13] EPEX SPOT, <https://www.epexspot.com>, accessed: 2019-12-31.
- [14] S. Voronin, J. Partanen, Price forecasting in the day-ahead energy market by an iterative method with separate normal price and price spike frameworks, *Energies* 6 (11) (2013) 5897–5920.
- [15] B. Tranberg, A. Thomsen, R. Rodriguez, G. Andresen, M. Schäfer, M. Greiner, Power flow tracing in a simplified highly renewable European electricity networks, *New Journal of Physics* 17 (2015) 105002. [doi:10.1088/1367-2630/17/10/105002](https://doi.org/10.1088/1367-2630/17/10/105002).
- [16] B. Tranberg, O. Corradi, B. Lajoie, T. Gibon, I. Staffell, G. B. Andresen, Real-time carbon accounting method for the European electricity markets, *Energy Strategy Reviews* 26 (2019) 100367. [doi:10.1016/j.esr.2019.100367](https://doi.org/10.1016/j.esr.2019.100367).
- [17] A. Finenko, L. Cheah, Temporal CO₂ emissions associated with electricity generation: Case study of Singapore, *Energy Policy* 93 (2016) 70–79.
- [18] K. Mason, J. Duggan, E. Howley, Forecasting energy demand, wind generation and carbon dioxide emissions in ireland using evolutionary neural networks, *Energy* 155 (2018) 705–720.
- [19] J. Krzywanski, T. Czakiert, A. Blaszcuk, R. Rajczyk, W. Muskala, W. Nowak, A generalized model of SO₂ emissions from large-and small-scale CFB boilers by artificial neural network approach: Part 1. The mathematical model of SO₂ emissions in air-firing, oxygen-enriched and oxycombustion CFB conditions, *Fuel Processing Technology* 137 (2015) 66–74.

- [20] Y. Bai, Y. Li, X. Wang, J. Xie, C. Li, Air pollutants concentrations forecasting using back propagation neural network based on wavelet decomposition with meteorological conditions, *Atmospheric Pollution Research* 7 (3) (2016) 557–566.
- [21] F. Biancofiore, M. Verdecchia, P. Di Carlo, B. Tomassetti, E. Aruffo, M. Busilacchio, S. Bianco, S. Di Tommaso, C. Colangeli, Analysis of surface ozone using a recurrent neural network, *Science of the Total Environment* 514 (2015) 379–387.
- [22] J. Chen, C. Gerbig, J. Marshall, K. U. Totsche, Short-term forecasting of regional biospheric co₂ fluxes in europe using a light-use-efficiency model, *Geoscientific Model Development Discussions* (2019) 1–26.
- [23] G. Lowry, Day-ahead forecasting of grid carbon intensity in support of heating, ventilation and air-conditioning plant demand response decision-making to reduce carbon emissions, *Building Services Engineering Research and Technology* 39 (6) (2018) 749–760.
- [24] N. E. Huang, Z. Shen, S. R. Long, M. C. Wu, H. H. Shih, Q. Zheng, N.-C. Yen, C. C. Tung, H. H. Liu, The empirical mode decomposition and the hilbert spectrum for nonlinear and non-stationary time series analysis, *Proceedings of the Royal Society of London. Series A: Mathematical, Physical and Engineering Sciences* 454 (1971) (1998) 903–995.
- [25] J. Dong, W. Dai, L. Tang, L. Yu, Why do emd-based methods improve prediction? a multiscale complexity perspective, *Journal of Forecasting* 38 (7) (2019) 714–731.
- [26] Y. Xu, J. Zhang, Z. Long, Y. Chen, A novel dual-scale deep belief network method for daily urban water demand forecasting, *Energies* 11 (5) (2018) 1068.
- [27] H. Liu, C. Chen, H.-q. Tian, Y.-f. Li, A hybrid model for wind speed pre-

- diction using empirical mode decomposition and artificial neural networks, *Renewable Energy* 48 (2012) 545–556.
- [28] Z. Wu, N. E. Huang, Ensemble empirical mode decomposition: a noise-assisted data analysis method, *Advances in Adaptive Data Analysis* 1 (01) (2009) 1–41.
- [29] N. Bokde, A. Feijóo, K. Kulat, Analysis of differencing and decomposition preprocessing methods for wind speed prediction, *Applied Soft Computing* 71 (2018) 926–938.
- [30] Z. Wu, N. E. Huang, X. Chen, The multi-dimensional ensemble empirical mode decomposition method, *Advances in Adaptive Data Analysis* 1 (03) (2009) 339–372.
- [31] N. Bokde, A. Feijóo, D. Villanueva, K. Kulat, A review on hybrid empirical mode decomposition models for wind speed and wind power prediction, *Energies* 12 (2) (2019) 254.
- [32] J. Zhou, X. Yu, X. Yuan, Predicting the carbon price sequence in the shenzhen emissions exchange using a multiscale ensemble forecasting model based on ensemble empirical mode decomposition, *Energies* 11 (7) (2018) 1907.
- [33] X. Zhang, K. K. Lai, S.-Y. Wang, A new approach for crude oil price analysis based on empirical mode decomposition, *Energy Economics* 30 (3) (2008) 905–918.
- [34] P. L. Barnard, D. Hoover, D. M. Hubbard, A. Snyder, B. C. Ludka, J. Allan, G. M. Kaminsky, P. Ruggiero, T. W. Gallien, L. Gabel, et al., Extreme oceanographic forcing and coastal response due to the 2015–2016 el niño, *Nature Communications* 8 (1) (2017) 1–8.
- [35] K. Dube, G. Nhamo, Climate variability, change and potential impacts on tourism: Evidence from the zambian side of the victoria falls, *Environmental Science & Policy* 84 (2018) 113–123.

- [36] R. J. Hyndman, Y. Khandakar, et al., Automatic time series for forecasting: the forecast package for R, no. 6/07, Monash University, Department of Econometrics and Business Statistics . . . , 2007.
- [37] N. Bokde, G. Asencio-Cortes, F. Martinez-Alvarez, PSF: Forecasting of Univariate Time Series Using the Pattern Sequence-Based Forecasting (PSF) Algorithm, R package version 0.4.
- [38] N. Bokde, G. Asencio-Cortés, F. Martínez-Álvarez, K. Kulat, PSF: Introduction to R Package for Pattern Sequence Based Forecasting Algorithm, *The R Journal* 9 (1) (2017) 324–333.
- [39] ENTSO-E Transparency Platform, <https://transparency.entsoe.eu>, accessed: 2019-12-31.
- [40] Tomorrow, electricityMap, <https://www.electricitymap.org>, accessed: 2019-12-31.
- [41] J.-L. Fan, Y.-B. Hou, Q. Wang, C. Wang, Y.-M. Wei, Exploring the characteristics of production-based and consumption-based carbon emissions of major economies: A multiple-dimension comparison, *Applied Energy* 184 (2016) 790–799.
- [42] Z. Zhang, J. Lin, From production-based to consumption-based regional carbon inventories: Insight from spatial production fragmentation, *Applied Energy* 211 (2018) 549–567.
- [43] J. Clauß, S. Stinner, C. Solli, K. B. Lindberg, H. Madsen, L. Georges, A generic methodology to evaluate hourly average co₂eq. intensities of the electricity mix to deploy the energy flexibility potential of norwegian buildings, in: *Proceedings of the 10th International Conference on System Simulation in Buildings*, Liege, Belgium, 2018, pp. 10–12.
- [44] M. Agenis, N. Bokde, [GuessCompX: Empirically Estimates Algorithm Complexity](#), R package version 1.0.3 (2019).
URL <https://CRAN.R-project.org/package=GuessCompX>

- [45] M. Agenis-Nevers, N. D. Bokde, Z. M. Yaseen, M. Shende, An empirical estimation for time and memory algorithm complexities: Newly developed R package, Multimedia Tools and Application In Press.
- [46] N. D. Bokde, Z. M. Yaseen, G. B. Andersen, Forecasttb—an r package as a test-bench for time series forecasting—application of wind speed and solar radiation modeling, *Energies* 13 (10) (2020) 2578.
- [47] N. D. Bokde, G. B. Andersen, [ForecastTB: Test Bench for the Comparison of Forecast Methods](#), R package version 1.0.1 (2020).
URL <https://CRAN.R-project.org/package=ForecastTB>